

# One Perturbation is Enough: On Generating Universal Adversarial Perturbations against Vision-Language Pre-training Models

Hao Fang<sup>1†</sup> Jiawei Kong<sup>2†</sup> Wenbo Yu<sup>2</sup> Bin Chen<sup>2#</sup> Jiawei Li<sup>3</sup> Shu-Tao Xia<sup>1</sup> Ke Xu<sup>4</sup>

<sup>1</sup>Tsinghua Shenzhen International Graduate School, Tsinghua University

<sup>2</sup>School of Computer science and Technology, Harbin Institute of Technology, Shenzhen

<sup>3</sup>Huawei Technology <sup>4</sup>Department of Computer Science and Technology, Tsinghua University

fang-h23@mails.tsinghua.edu.cn, {kongjiawei, yuwenbo}@stu.hit.edu.cn, chenbin2021@hit.edu.cn

li-jw15@tsinghua.org.cn, xiast@sz.tsinghua.edu.cn, xuke@tsinghua.edu.cn;

**Abstract**—Vision-Language Pre-training (VLP) models trained on large-scale image-text pairs have demonstrated unprecedented capability in many practical applications. However, previous studies have revealed that VLP models are vulnerable to adversarial samples crafted by a malicious adversary. While existing attacks have achieved great success in improving attack effect and transferability, they all focus on instance-specific attacks that generate perturbations for each input sample. In this paper, we show that VLP models can be vulnerable to a new class of universal adversarial perturbation (UAP) for all input samples. Although initially transplanting existing UAP algorithms to perform attacks showed effectiveness in attacking discriminative models, the results were unsatisfactory when applied to VLP models. To this end, we revisit the multimodal alignments in VLP model training and propose the Contrastive-training Perturbation Generator with Cross-modal conditions (C-PGC). Specifically, we first design a generator that incorporates cross-modal information as conditioning input to guide the training. To further exploit cross-modal interactions, we propose to formulate the training objective as a multimodal contrastive learning paradigm based on our constructed positive and negative image-text pairs. By training the conditional generator with the designed loss, we successfully force the adversarial samples to move away from its original area in the VLP model’s feature space, and thus essentially enhance the attacks. Extensive experiments show that our method achieves remarkable attack performance across various VLP models and Vision-and-Language (V+L) tasks. Moreover, C-PGC exhibits outstanding black-box transferability and achieves impressive results in fooling prevalent large VLP models including LLaVA and Qwen-VL.

## 1. Introduction

Vision-Language Pre-training (VLP) models [1], [2], [3] have recently demonstrated remarkable efficacy in many downstream Vision-and-Language (V+L) tasks, such as

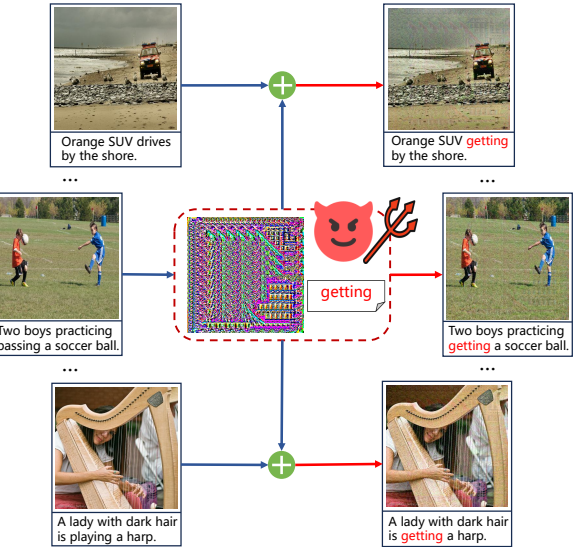


Figure 1. Illustration of the universal adversarial attacks against VLP models. With only a pair of image-text perturbations, the proposed attack can effectively mislead different models on diverse V+L tasks.

image-text retrieval [4], visual grounding [5], and visual entailment [6]. By self-supervised pre-training on large-scale unlabeled image-text pairs, the VLP model efficiently aligns cross-modal features and captures rich information from aligned multimodal embeddings, thereby providing expressive representations for downstream applications.

Adversarial attacks [7], [8], which aim to deceive models during inference time, have attracted extensive attention in recent years due to their significant threat to security-critical scenarios including automatic driving [9], financial systems [10], and face recognition [11]. A series of recent studies have shown that VLP models are also vulnerable to adversarial samples. The pioneering work Co-Attack [12] proposes the first multimodal adversarial attack that simultaneously perturbs both image and text modalities. Although Co-Attack displays excellent attack performance, it only considers relatively easier white-box attacks where victim models are completely accessible to the adversary. To handle more practical black-box settings, subsequent studies pro-

<sup>†</sup>The two authors contribute equally to this work.

<sup>#</sup>Corresponding Author

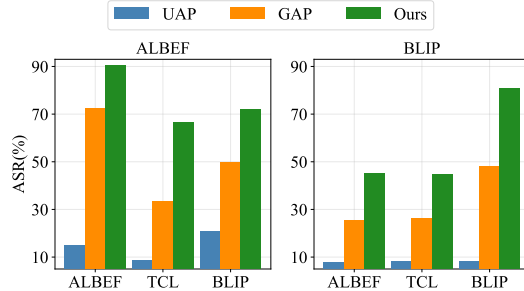


Figure 2. Performance of existing universal adversarial attacks on the text retrieval task. We transplant UAP [15] and GAP [16] to fool VLP models. The surrogate models are ALBEF [1] and BLIP [18]. We also present the results of our C-PGC for comparison.

pose various transferability-based black-box methods that transfer adversarial samples generated by an available surrogate model to fool other inaccessible models. Specifically, SGA [13] significantly improves the adversarial transferability of crafted image-text adversarial examples through set-level cross-modal guidance obtained from data augmentations. Considering the underlying mechanism of VLP models during decision-making, TMM [14] jointly destroys the modality-consistency features within the clean image-text pairs and includes more modality-discrepancy features in the adversarial perturbations. This strategy successfully confuses VLP models and achieves outstanding transferability. Despite the great efforts and success in enhancing attacks on VLP models, these methods are all instance-specific attacks that require generating an adversarial perturbation for each input pair. Meanwhile, universal adversarial attacks, as a typical efficient instance-agnostic approach that uses only one Universal Adversarial Perturbation (UAP) to conduct the attacks, have exhibited remarkable performance in fooling classification tasks [15], [16], [17]. None of these works theoretically or empirically demonstrate the vulnerability of VLP models under UAP. This naturally leads to a question, *is it possible to design a universal adversarial perturbation that can effectively deceive VLP models?*

**Motivation.** To address this question, we conduct a deep exploration of this challenging topic. First, we made an intuitive attempt that transplants existing UAP generation approaches [15], [16] to launch attacks on VLP models by replacing the traditional cross-entropy loss with the cosine distance [13] between the embeddings of the adversarial image and its corresponding matched texts. Unfortunately, experimental results in Figure 2 demonstrate that these UAP methods yield unsatisfactory attack success rates (ASR) when targeting VLP models. Empirically, the main reason for the failure is that these attacks narrowly target the single image modality, totally disregarding the other modality and the multimodal information, which plays a crucial role in the VLP models. To overcome this challenge, we revisit the basic training paradigm of VLP models and emphasize that regardless of the downstream V+L tasks, the outstanding performance achieved by these models is largely attributed to the successful vision-language feature alignment mechanism, which draws the embedding of matched image-text

pairs closer while distancing those of non-matched pairs. In light of this consideration, we argue that the key core of an effective attack against VLP models is to obtain adversarial examples that can fundamentally destroy the learned alignment relationship. i.e., making the embedding of the generated adversarial example keep distance from its matched counterparts as far as possible to mislead VLP models into making incorrect decisions. Therefore, we aim to seek a UAP that can yield a significant discrepancy in the embedding space when added to the matched image-text pair. Besides, previous studies have revealed that in the context of V+L scenarios, the joint attack of both modalities (image&text) consistently outperforms solely perturbing data from a single modality [12], [13], [14]. Accordingly, the designed UAP is expected to perturb both image and text modalities simultaneously. Another notable phenomenon in Figure 2 is that using a generator could improve the ASR of the crafted UAP. This is also verified by numerous previous studies [16], [19]. Hence, it could be a better choice to adopt a generator-based UAP approach.

**Our contributions.** Based on these insights, we propose a generative framework, which learns a Contrastive-training Perturbation Generator with Cross-modal conditions (C-PGC), to produce UAP for attacking VLP models. By contrastive training C-PGC with our maliciously constructed positive and negative image-text pairs, the generated UAP pushes the embedding of matched image-text pairs apart while pushing those of non-matched pairs together, thus effectively perturbing the multimodal feature alignment. In addition, we also consider the intra-modal influence and introduce a distance loss to further enhance the attacks. For the case of image modality, we maximize the Euclidean distance between the embedding of the adversarial image and the original clean sample to push the adversarial image away from its original feature area. Then, we propose a novel cross-modal conditioned generator to better capture the data distribution and cross-modal interactions for enhanced generalization of the UAP. By optimizing our carefully designed modality-aware generator with the contrastive loss, the input fixed noise is transformed into the UAP that can generalize across various samples and networks. Moreover, we generate UAPs for both image and text to exploit the synergy between different modalities to strengthen the attacks further.

To reveal the excellent performance of our proposed method, we conduct thorough experiments on various prevalent VLP models (e.g., ALBEF, TCL, CLIP, and BLIP) across a wide range of V+L tasks, including image-text retrieval, image captioning, visual grounding, and visual entailment. Apart from white-box scenarios, we also discuss the more practical and challenging black-box attacks. Taking different VLP models as surrogates, we generate UAPs to fool other unknown black-box models to show the outstanding transferability of our proposed method. In addition, we demonstrate the robustness of our C-PGC under a variety of defense strategies, including the SOTA diffusion-based purification defense. Furthermore, we highlight that we launch transferable black-box attacks on multiple Large vision-language Models (LVLM), such as Qwen-VL [20]

and LLaVA [21]. The impressive attack effects raise new security concerns during the model’s inference stage in this distinctive era of LVLM evolution and explosion.

Our contributions can be summarized as follows:

- To the best of our knowledge, we are the first to exploit both image and text modalities to conduct UAP attacks against VLP models. We show that even though using only one universal perturbation, our method can induce a serious performance degradation to the attacked VLP models.
- We propose a generative UAP framework, which incorporates rich information from both unimodal and multimodal features to guide the contrastive training of the generator for improved attacks.
- We conduct exhaustive experiments on 6 various VLP models across different V+L tasks. Extensive results reveal that our method achieves outstanding performance and excellent black-box transferability (Sec. 5.2, 5.4). C-PGC exhibits impressive transferability to multiple mainstream LVLMs (Sec. 5.4) and robustness under 8 considered defenses (Sec. 6).
- The proposed work holds strong practical significance due to its exceptional attack effects across diverse settings, which renders it a reliable tool for evaluating the adversarial robustness of VLP models.

## 2. Background

### 2.1. Basis of VLP Models

Vision-Language Pre-training (VLP) models are pre-trained on massive image-text pairs to learn the semantic correlations across modalities and serve for diverse multimodal user demands [22], [23]. We next illustrate the basis of VLP models from multiple perspectives.

**Extraction and Representation of Features.** As for text feature extraction, similar to well-known pre-trained language models (e.g., BERT [24]), VLP models first split the input texts into a series of subwords with a start-of-sequence token [SOS] and an end-of-sequence token [EOS] respectively inserted to the beginning and the end [25], [26], [27]. Then, the textual representations are computed by combining the word embeddings, the positional embeddings, and the type embeddings. As for image feature extraction, VLP models exploit different types of neural networks to obtain different levels of features. Specifically, some propose to extract region-level features by pre-trained object detectors [25], [28], [29], some propose to extract grid-level features via convolutional neural networks (CNNs) [30], [31], and some others propose to extract patch-level features through Vision Transformer (ViT) [32], [33].

**Architectures.** Based on the ways of multimodal fusion, the architectures of VLP models can be classified into two types: *single-stream architectures* and *dual-stream architectures*. Single-stream architectures [25], [34], [35] directly concatenate the text and image features, and calculate the attention in the same Transformer block for multimodal

fusion. On the contrary, dual-stream architectures [36], [37] do not conduct such concatenation. They separately send the text and image features to different Transformer blocks and leverage the cross-attention mechanism for multimodal fusion. In comparison, single-stream architectures are more parameter-efficient than dual-stream architectures since they adopt the same set of parameters in a Transformer block for the text and image modalities. Furthermore, the architectures of VLP models can also be divided into *encoder-only architectures* and *encoder-decoder architectures*. Encoder-only architectures directly send the multimodal representations to the output layer, while encoder-decoder architectures first send the multimodal representations to a decoder before feeding them into the output layer.

**Pre-training Objectives.** The pre-training objectives for VLP models mainly include *masked features completion*, *multimodal features matching*, and *specific downstream objectives*. Masked features completion [34], [38], [39] refers to that some of the textual or vision tokens are deliberately masked, and VLP models will try to predict these masked tokens from the remaining unmasked tokens during pre-training. Thus, VLP models can promote the understanding of multimodal data when learning from the completion. To tackle the high-dimensional and continuous characteristics of vision data, VLP models adopt two variants of completion when predicting vision tokens, namely masked features regression [40], [41], [42] and masked features classification [28], [34], [43]. Multimodal features matching [1], [33], [44] refers to that VLP models learn to precisely predict whether the image-text pairs are matched or mismatched during pre-training. In this way, the textual and vision features can be fully aligned by the VLP models. Specific downstream objectives [45], [46], [47] indicate that VLP models directly utilize the training objectives of downstream tasks (e.g., visual question answering) for pre-training. By doing so, VLP models can better adapt to various downstream tasks.

**Downstream Tasks.** VLP models have a wide range of practical applications. In this paper, we mainly consider the above multimodal downstream tasks: (1) Image-text retrieval (ITR) [4], [48], [49]: finding the most matched image for the given text and vice versa, and can be further split into image-to-text retrieval (TR) and text-to-image retrieval (IR). (2) Image caption (IC) [50], [51], [52]: generating the most suitable descriptions for the given image. (3) Visual grounding (VG) [5], [53], [54]: locating specific regions in the image that correspond with the given textual descriptions. (4) Visual entailment (VE) [3], [6], [55]: analyzing the input image and text, and predicting whether the relationship between them is entailment, neutral or contradiction.

### 2.2. Adversarial Attacks on VLP Models

The adversarial robustness of VLP Models has already become a research focus. Early works [56], [57], [58], [59] only impose perturbations on one single modality (e.g., image or text modality) and severely lack cross-modal interactions when attacking multimodal models. To alleviate this issue, Zhang *et al.* [12] propose Co-Attack and firstly

conduct multimodal adversarial attacks on VLP models under white-box settings. They comprehensively consider the consistency between different modalities and induce the image-text perturbations towards a stronger attack. On the basis of Co-Attack, Lu *et al.* [13] extend the attacks to more rigorous black-box settings and propose SGA, which utilizes set-level alignment-preserving argumentations with carefully designed cross-modal guidance. By enriching the aligned image-text pairs, SGA significantly boosts the black-box adversarial transferability across different VLP models. However, Wang *et al.* [14] point out that the simple interaction mechanism of SGA actually fails to fully exploit modality correlation, and propose TMM to better leverage cross-modal interactions by tailoring both the modality-consistency and modality-discrepancy features. The adversarial attacks mentioned above, whether transferable or not, are all instance-specific attacks. Instance-specific attacks redesign the perturbations for each pair of input samples. In this paper, we make a step forward and manage to generate instance-agnostic UAPs for VLP models.

### 3. Threat Model

In this section, we elaborated on the threat model of the proposed C-PGC from three perspectives including the goal, knowledge, and capability of the attacker.

#### 3.1. Adversary Goal

The attacker’s objective is to craft a pair of universal adversarial perturbations for both image and text modalities that are capable of deceiving the VLP models and ultimately leading to prediction errors in downstream V+L tasks. To ensure the stealthiness of the attacks, the adversary seeks to obtain an imperceptible perturbation by imposing additional constraints on the generated perturbation regarding its range or magnitude. On the premise of guaranteeing the concealment of the generated perturbation, attackers aim to generalize the crafted UAP to a wider range of data and victim models.

#### 3.2. Adversary Knowledge

Similar to previous UAP algorithms [15], [16], we assume that attackers possess a certain quantity of samples from an available dataset to learn the universal perturbation. Nevertheless, it is assumed that they do not have any prior knowledge of the test data that are used to add the perturbation and attack the VLP models. The evaluated samples may either adhere to the identical (same-domain scenarios) or a different distribution (cross-domain scenarios) from the distribution of UAP’s training samples. For instance, an adversary might generate a UAP leveraging image-text pairs from the MSCOCO dataset, whereas the attacks would be actually conducted on data from the Flickr30k. Note that this cross-domain scenario is considerably challenging since the UAP highly depends on the training data and thus it requires exceptional cross-domain transferability to successfully perform the attacks.

### 3.3. Adversary Capability

We discuss two distinct attack settings. In each setting, the adversary has different levels of access to the target VLP models and auxiliary information.

**White-box.** White-box settings indicate that the adversary has complete accessibility to the target model including the model’s parameters, gradients, and outputs, which can be leveraged to significantly boost the attack effects. This white-box setting is too ideal in realistic scenarios.

**Black-box.** We mainly focus on the black-box setup where the adversary is only capable of making queries to an unknown VLP model. Specifically, we consider a more efficient black-box paradigm, i.e., the transferable adversarial attack which involves producing the UAP on a publicly available white-box model and then directly feeding the corresponding adversarial samples to other black-box models.

## 4. Universal Multimodal Attacks

In this section, we first present the problem statement of universal adversarial attacks on VLP models. Next, we introduce the overview of our framework and the detailed design of each proposed technique. Finally, we summarize the training objective and paradigm of C-PGC.

### 4.1. Problem Statement

We define the image-text pair as  $(\mathbf{v}_i, \mathbf{t}_i)$  and denote  $\mathbf{e}_v$  and  $\mathbf{e}_t$  as the image and text embedding encoded by the image encoder  $f_I(\cdot)$  and text encoder  $f_T(\cdot)$  of a targeted VLP model  $f(\cdot)$ . The goal of multimodal universal adversarial attacks is to generate a pair of image-text perturbations  $(\delta_v, \delta_t)$  that can affect a vast majority of samples from the target dataset  $\mathcal{D}_t$  to deceive downstream V+L tasks into making incorrect decisions. To guarantee the imperceptibility of perturbations, we must carefully constrain the pixel-level image perturbation with  $l_\infty$  norm of a given budget  $\epsilon_v$ . Our work adopts the standard setting [14] with the  $\epsilon_v$  value of 12/255. For text modality, we employ the same perturbation strategy as prior attacks on VLP models [12], [13], [14], i.e., replacing certain important tokens of the original text description with the crafted adversarial words. Accordingly, the textual perturbation is token-level and constrained by the number of modified words  $\epsilon_t$ . Since altering words in a natural sentence can be easily noticed or detected, we apply a rigorous restriction that only permits a single word to be substituted within one sentence ( $\epsilon_t = 1$ ). Let  $\mathcal{D}_t$  be an available dataset consisting of image-text pairs collected by an attacker, then he adopts a generator  $G(\cdot)$  learned on the given training dataset  $\mathcal{D}_t$  to produce the UAP.

### 4.2. Overview of the Framework

As depicted in Figure 3, we generate perturbations for image and text modalities respectively. Since the key workflows for image and text modalities are symmetrical with

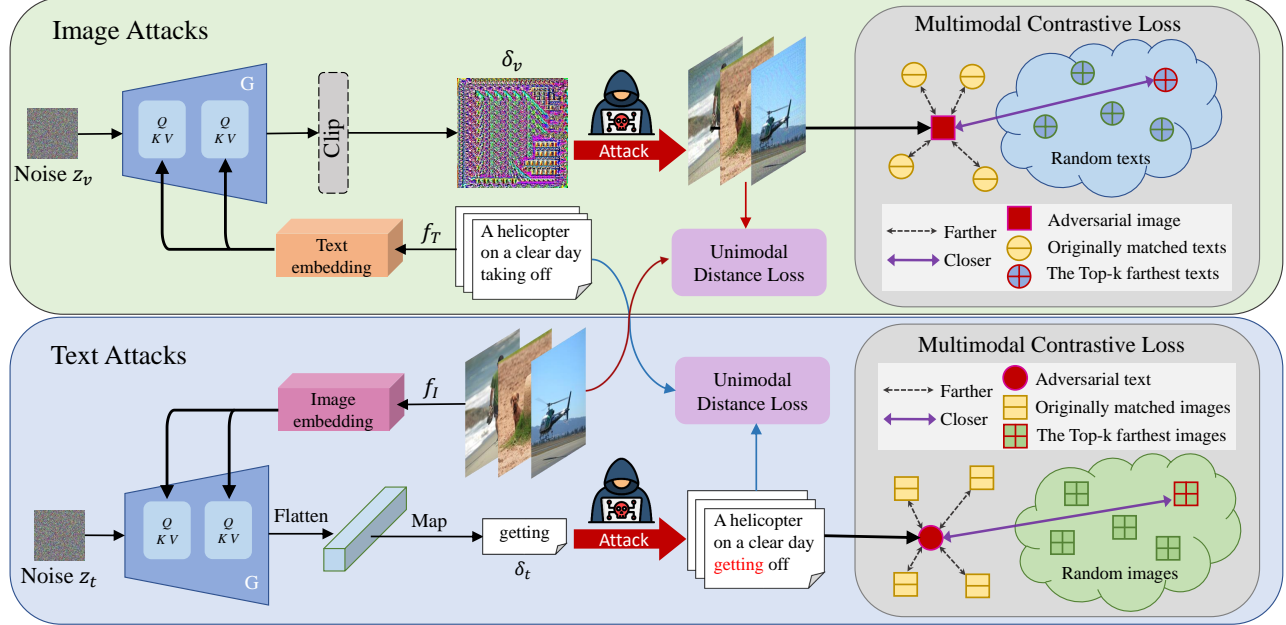


Figure 3. An overview of our proposed universal adversarial attack framework. Benefiting from the well-designed unimodal distance loss  $\mathcal{L}_{dis}$  and multimodal contrastive loss  $\mathcal{L}_{CL}$ , the conditional generator learns rich knowledge from features of different modalities and thus respectively produce UAP  $\delta_v$  and  $\delta_t$  with superior attack effects and adversarial transferability across diverse models and down-stream tasks.

each other, below we take the image attacks as an example to illustrate the proposed framework.

A fixed noise  $\mathbf{z}_v$  is first randomly initialized and subsequently fed into the conditional generator. Given a data pair  $(\mathbf{v}, \mathbf{t})$ , the conditional generator  $G(\cdot)$  then translates the input noise  $\mathbf{z}_v$  into the adversarial perturbation  $\delta_v$  that is of the same size as the image  $\mathbf{v}$  and under a budget of  $\epsilon_v$ . During the process of the perturbation generation, the network  $G$  additionally benefits from cross-modal information by integrating textual information as conditioning inputs through the advanced cross-attention mechanism. Next, the generated adversarial noise  $\delta_v$  is injected into the clean image to obtain the adversarial image, i.e.,  $\mathbf{v}_{adv} = \mathbf{v} + \delta_v$ . To better guide the training process, we design two efficient unimodal and multimodal losses as our optimization objectives. Unimodal loss is straightforward and aims to push the adversarial images away from the clean images in the latent embedding space, while multimodal loss is based on contrastive learning and uses our manually constructed positive and negative sample to effectively destroy the image-text embeddings' matching relationship obtained from feature alignment. Once we finish training the C-PGC using the proposed multimodal and unimodal losses, the input fixed noise is transformed into a UAP that is of great generalization and transferability.

### 4.3. Detailed Design of C-PGC

Next, we provide a detailed introduction to each of the proposed designs. Note that we also discuss attacking the image modality as an example, given that the design of the text attack is completely symmetrical. The pseudocode of the training procedure is provided in Alg. 1 of Appendix A.

**Perturbation Generator with Cross-modal conditions.** Previous generative universal adversarial attacks [16] have demonstrated excellent performance in fooling the discriminative models. However, the used generator is limited to a single modality, whereas multimodal interactions play a critical role in VLP models. To fill this gap, we leverage cross-modal embeddings as conditioning inputs for the perturbation generator. Specifically, we introduce the condition inputting mechanism by adding the advanced cross-attention modules that have been proven effective in tasks with variable input modalities. Specifically, we incorporate textual embeddings  $e_t$  from the VLP model's latent space into our generator through a cross-attention layer:

$$Q = \mathbf{h}_t W_q, K = e_t W_k, V = e_t W_v, \\ \text{Attention}(Q, K, V) = \text{softmax}\left(\frac{QK^T}{\sqrt{d}}\right) \cdot V, \quad (1)$$

where  $\mathbf{h}_t \in \mathbb{R}^{B \times d_\alpha}$  is the flattened intermediate features within the generator,  $W_q \in \mathbb{R}^{d_\alpha \times d}$ ,  $W_k \in \mathbb{R}^{512 \times d}$ ,  $W_v \in \mathbb{R}^{512 \times d}$  are optimized parameters.

**Multimodal Contrastive Loss.** The preceding in-depth analysis regarding the failures of existing UAP attacks encourages us to design a loss that can guide the generated UAP to essentially break the multimodal feature alignment. In light of the success of contrastive learning in VLP models, we adopt the widely recognized and effective contrastive loss InfoNCE [60] as our basic loss function.

We let the adversarial image  $\mathbf{v}_{adv}$  serve as the anchor sample. To formulate the InfoNCE loss, it is necessary to construct an appropriate set of positive and negative samples. Based on the fundamental objective of our attacks, it is natural that the originally matched texts set

$\mathcal{T} = \{\mathbf{t}_1, \mathbf{t}_2 \dots, \mathbf{t}_M\}$  can be employed as negative samples  $\mathbf{t}_{neg}$  to increase their discrepancy in the feature space of VLP models. To further push the adversarial image  $\mathbf{v}_{adv}$  away from its correct text descriptions  $\mathbf{t}$ , we propose utilizing multiple texts whose embeddings differ significantly from that of the original clean images  $\mathbf{v}$  as the positive sample  $\mathbf{t}_{pos}$ . Specifically, we randomly sample a batch of text descriptions from  $\mathcal{D}_s$  and select the texts with Top-K feature distances from the clean image  $\mathbf{v}$  as positive samples, i.e.,  $\mathcal{T}_{pos} = \{\mathbf{t}'_1, \mathbf{t}'_2 \dots, \mathbf{t}'_K\}$ . Moreover, we follow SGA and utilize data augmentations that resize the image  $\mathbf{v}$  into different scales and apply random Gaussian noise to acquire more diverse set-level guidance. Using the obtained image set  $\mathcal{V} = \{\mathbf{v}_1, \mathbf{v}_2 \dots, \mathbf{v}_S\}$  and these well-constructed positive and negative samples, the cross-modal contrastive loss  $\mathcal{L}_{CL}$  can be formulated as:

$$\mathcal{L}_{CL} = \log \left( \frac{\sum_{i=1}^S \sum_{j=1}^M e^{d(\mathbf{v}_i + \delta_v, \mathbf{t}_j) / \tau}}{\sum_{i=1}^S \sum_{j=1}^M e^{d(\mathbf{v}_i + \delta_v, \mathbf{t}_j) / \tau} + \sum_{i=1}^S \sum_{j=1}^K e^{d(\mathbf{v}_i + \delta_v, \mathbf{t}'_j) / \tau}} \right), \quad (2)$$

where  $\delta_v$  is the universal perturbation,  $\tau$  denotes the temperature parameter and  $d(\mathbf{v}, \mathbf{t}) = \text{Sim}(f_I(\mathbf{v}), f_T(\mathbf{t}))$ , where  $\text{Sim}(\cdot, \cdot)$  represents the cosine similarity measurement.

**Unimodal Distance Loss.** Given an image-text pair  $(\mathbf{v}, \mathbf{t})$ , previous studies on contrastive learning [2] usually apply separate augmentations to the image  $\mathbf{v}$  to obtain several views of  $\mathbf{v}$  and then construct positive pairs using  $\mathbf{v}$  and its augmented images. Inspired by this operation, an adversary can maliciously leverage a similar method to further promote the attack effects. Concretely, the input image  $\mathbf{v}$  is initially resized to different scales and then added with Gaussian noise to generate the image set  $\mathcal{V} = \{\mathbf{v}_1, \mathbf{v}_2 \dots, \mathbf{v}_S\}$ . Then, we craft the adversarial image through  $\mathbf{v}_{adv} = \mathbf{v} + \delta_v$  and process  $\mathbf{v}_{adv}$  with the same augmentation operation to obtain the adversarial image set  $\mathcal{V}_{adv} = \{\mathbf{v}'_1, \mathbf{v}'_2 \dots, \mathbf{v}'_S\}$ . Finally, we minimize the Euclidean distance between the encoded embeddings of adversarial images and clean images to learn the UAP that can push the adversarial images away from their initial visual semantic area. The loss  $\mathcal{L}_{dis}$  is formulated as:

$$\mathcal{L}_{dis} = - \sum_{i=1}^S \sum_{j=1}^S \|\mathbf{f}_I(\mathbf{v}'_i) - \mathbf{f}_I(\mathbf{v}_j)\|_2 \quad (3)$$

Taking advantage of the unimodal set-level guidance,  $\mathcal{L}_{dis}$  ensures an effective optimization direction during the generator training and further enhances the attacks.

**Attacking Text Modality.** As aforementioned, the generator's structure and training losses for textual attacks are completely symmetrical with the design of the image attacks. Given an adversarial text  $\mathbf{t}_{adv}$  as the anchor sample, we use the set  $\mathcal{V} = \{\mathbf{v}_1, \mathbf{v}_2 \dots, \mathbf{v}_S\}$  scaled from the originally matched image  $\mathbf{v}$  as negative while the  $\mathcal{V}' = \{\mathbf{v}'_1, \mathbf{v}'_2 \dots, \mathbf{v}'_S\}$  scaled from the farthest image  $\mathbf{v}'$  within the randomly sampled set as positive samples to formulate the  $\mathcal{L}_{CL}$  loss.  $\mathcal{L}_{dis}$  is then calculated as the Euclidean

distance between the embedding of  $\mathbf{t}_{adv}$  and the clean input  $\mathbf{t}$ . Besides, the perturbation generator is correspondingly conditioned with the embedding of the matched image  $\mathbf{v}$ .

A notable distinction between the image and text attacks is the approach to inject adversarial perturbations. Due to the discreteness of the text data, we apply the token-wise substitute perturbation strategy [13], [14] that replaces certain important words in the original sentence with crafted adversarial words. Accordingly, the conditional generator is utilized to output the adversarial textual embeddings, which are subsequently mapped back to the vocabulary space to obtain a universally applicable word-level perturbation. Prior to implementing the word replacement, a meticulous process is undertaken to identify the most optimal position within the sentence to insert the perturbation. Our strategy intends to identify and replace the words that are more likely to have a greater influence on the model's decision-making process. Specifically, for each word  $w_i$  within a given sentence, we compute the distance between the embeddings of original sentence and the  $w_i$ -masked version encoded by the VLP models to determine its contribution to the whole sentence. To ensure the attack stealthiness, we set  $\epsilon_t = 1$  and choose the single word exerting the highest feature distance is selected as the target for replacement.

#### 4.4. Training Objective

Consider the case of image attacks. For each given input pair  $(\mathbf{v}, \mathbf{t})$ , we first generate the UAP via  $\delta_v = G(\mathbf{z}_v; \mathbf{t})$  and obtain the adversarial image by  $\mathbf{v}_{adv} = \mathbf{v} + \delta_v$ . Then we calculate the proposed  $\mathcal{L}_{dis}$  using  $\mathbf{v}$  and  $\mathbf{v}_{adv}$ , and the contrastive loss  $\mathcal{L}_{CL}$  using the constructed positive and negative samples. Based on the two loss terms, the overall optimization objective of our cross-modal conditional generator can be defined as:

$$\mathcal{L}_{total} = \mathcal{L}_{CL} + \alpha \mathcal{L}_{dis} \quad (4)$$

where  $\alpha$  is the pre-defined hyperparameter to balance the contributions of  $\mathcal{L}_{CL}$  and  $\mathcal{L}_{dis}$ , which is set to 0.1 by default and is proved to be the most effective one in our ablation study. By training the network using the proposed loss function based on the data distribution of the multimodal training dataset  $\mathcal{D}_s$ , the generator is encouraged to produce UAP that can push the features of mismatched image-text pairs together while pulling the embedding of the matched ones apart, thereby learning a UAP with excellent generalization and transferability.

#### 5. Evaluation

In this section, we first present detailed experimental settings in Sec. 5.1 and then provide a comprehensive evaluation of the proposed algorithm across different victim VLP models in Sec. 5.2. Subsequently, Sec. 5.3 includes sufficient ablation studies to validate the contribution of each proposed technique and explore the impact of several crucial factors on the attack effect. To further validate the effectiveness of



Figure 4. Illustration of Image retrieval tasks. The red indicates the universal adversarial word and the crossed-out word is the word to replace. We generate the UAP on the ALBEF model and test it on 6 different target models. It can be observed that all the retrieved images do not accurately correspond to the query text, verifying the outstanding attack ability of our method.

our proposed C-PGC, Sec. 5.4 presents results on diverse scenarios including more downstream V+L tasks, cross-domain attacks, and transfer to large VLP models.

## 5.1. Experimental Setup

**Downstream tasks and datasets.** We conduct a comprehensive study of C-PGC on four downstream V+L tasks, including image-text retrieval (ITR), image captioning (IC), visual grounding (VG), and visual entailment (VE). Their used datasets are as follows:

- **Flickr30K** [61]. Collected from the Flickr website, this dataset describes different items and activities, which becomes a standard benchmark for various V+L tasks. It contains 31,783 images, each of which has five associated captions. We use it for ITR tasks.
- **MSCOCO** [62]. The MSCOCO dataset is a rich and diverse dataset consisting of 123,287 images, each of which is annotated with approximately five sentences. We use this dataset to test the attack performance of ITR and IC tasks.
- **SNLI-VE** [6]. Originally proposed for natural language reasoning tasks, this dataset provides large-scale images and descriptions, where each image is annotated with several sentences and their logical relationship labels, including entailment, neutral, and contradiction. This dataset is used for VE tasks.
- **RefCOCO+** [63]. RefCOCO+ is an image dataset selected from MSCOCO. It contains 19,992 images and 141,564 annotations, which is specially used for visual grounding (VG) tasks.

**Surrogate models and victim models.** As for the ITR tasks, we adopt ALBEF [1], TCL [2], X-VLM [27], CLIP<sub>ViT</sub>

[33], CLIP<sub>CNN</sub> [33], and BLIP [18] as the surrogate models and victim models. Note that different image feature extraction modules are utilized for CLIP, namely ViT-B/16 for CLIP<sub>ViT</sub> and ResNet-101 for CLIP<sub>CNN</sub>, while in other models only ViT is leveraged for image feature extraction. More concretely, in ITR tasks we comprehensively consider the cases of adopting any one of these six models as the surrogate model and regarding any one of these six models as the victim model, thus there are 36 pairs of surrogate-victim models altogether. As for the IC tasks, we adopt ALBEF, TCL, and BLIP as the surrogate models and transfer the attacks to the commonly used captioning model BLIP. As for the VG tasks, we use ALBEF, TCL, and X-VLM as the surrogate models and victim models. As for the VE tasks, we leverage ALBEF and TCL as the source and target models. We also emphasize that among all the six given VLP models, only ALBEF, TCL and X-VLM can deal with VG tasks, while only ALBEF and TCL can deal with VE tasks.

**Metrics.** We regard the attack success rate (ASR) as the main quantitative metric when evaluating the effectiveness of our universal adversarial samples. This metric measures to what extent the adversarial perturbations on the victim models result in deviations from the correct decisions. In ITR tasks, R@1, R@5, and R@10 are commonly considered indicators when calculating ASR. Note that R@N represents the top N most matched text(s)/image(s) based on the given query image/text. Due to the space limit, we report the ASR with regards to R@1 for our main results in Table 1, and present the results about R@5 and R@10 in the Appendix. As for the other cross-modal downstream V+L tasks, including IC, VG, and VE, we will illustrate their evaluation metrics when reporting the corresponding experimental results in the latter section of this paper.

TABLE 1. ATTACK SUCCESS RATES (%) OF OUR C-PGC AND GAP FOR IMAGE-TEXT RETRIEVAL TASKS ON TWO LARGE DATASETS FLICKR30K AND MSCOCO. TR INDICATES TEXT RETRIEVAL BASED ON THE INPUT IMAGE, WHILE IR INDICATES IMAGE RETRIEVAL USING INPUT TEXT.

Dataset	Source	Method	ALBEF		TCL		X-VLM		CLIP <sub>VIT</sub>		CLIP <sub>CNN</sub>		BLIP	
			TR	IR	TR	IR	TR	IR	TR	IR	TR	IR	TR	IR
Flickr30k	ALBEF	GAP	72.46	82.69	33.23	38.82	11.08	22.67	42.86	49.92	55.96	62.39	49.63	53.31
		Ours	<b>90.24</b>	<b>89.51</b>	<b>66.67</b>	<b>69.59</b>	<b>31.4</b>	<b>44.75</b>	<b>60.84</b>	<b>73.56</b>	<b>74.22</b>	<b>81.62</b>	<b>72.13</b>	<b>73.84</b>
	TCL	GAP	39.88	45.89	84.2	80.34	11.18	22.52	41.38	50.88	53.76	63.45	47.11	51.62
		Ours	<b>57.86</b>	<b>62.99</b>	<b>95.45</b>	<b>91.57</b>	<b>22.36</b>	<b>39.66</b>	<b>62.32</b>	<b>74.45</b>	<b>72.54</b>	<b>80.92</b>	<b>63.62</b>	<b>68.96</b>
	X-VLM	GAP	28.06	34.40	27.12	34.87	80.35	76.91	48.52	54.19	62.69	66.11	43.95	47.96
		Ours	<b>36.18</b>	<b>55.06</b>	<b>40.06</b>	<b>57.63</b>	<b>93.70</b>	<b>92.2</b>	<b>65.64</b>	<b>72.63</b>	<b>76.3</b>	<b>81.06</b>	<b>61.09</b>	<b>68.25</b>
MSCOCO	CLIP <sub>VIT</sub>	GAP	26.82	35.50	34.47	42.28	21.75	33.4	81.63	83.91	49.61	60.71	34.38	42.30
		Ours	<b>41.62</b>	<b>50.58</b>	<b>50.83</b>	<b>55.89</b>	<b>34.65</b>	<b>46.06</b>	<b>89.04</b>	<b>93.59</b>	<b>64.77</b>	<b>75.42</b>	<b>50.16</b>	<b>57.89</b>
	CLIP <sub>CNN</sub>	GAP	20.94	37.88	30.27	44.44	27.13	35.29	27.83	43.22	76.11	85.2	34.07	43.5
		Ours	<b>29.09</b>	<b>49.13</b>	<b>36.85</b>	<b>54.15</b>	<b>29.37</b>	<b>50.22</b>	<b>39.9</b>	<b>64.75</b>	<b>82.12</b>	<b>88.94</b>	<b>38.80</b>	<b>56.89</b>
	BLIP	GAP	25.49	34.07	26.19	34.63	11.28	22.11	42.00	49.7	52.07	60.12	48.16	73.70
		Ours	<b>45.32</b>	<b>52.41</b>	<b>44.82</b>	<b>53.38</b>	<b>27.24</b>	<b>41.8</b>	<b>60.22</b>	<b>68.33</b>	<b>71.5</b>	<b>78.19</b>	<b>80.63</b>	<b>87.31</b>
MSCOCO	ALBEF	GAP	83.63	84.82	54.89	49.64	21.55	21.44	49.48	47.87	59.8	60.07	56.12	52.72
		Ours	<b>96.49</b>	<b>95.47</b>	<b>81.32</b>	<b>78.00</b>	<b>45.95</b>	<b>52.37</b>	<b>74.63</b>	<b>75.48</b>	<b>79.53</b>	<b>82.01</b>	<b>77.51</b>	<b>76.24</b>
	TCL	GAP	60.17	54.94	95.66	92.98	26.2	25.7	51.43	50.04	63.44	64.27	60.72	55.47
		Ours	<b>81.62</b>	<b>76.71</b>	<b>97.2</b>	<b>94.35</b>	<b>52.28</b>	<b>55.00</b>	<b>88.22</b>	<b>84.15</b>	<b>86.44</b>	<b>89.24</b>	<b>81.72</b>	<b>80.07</b>
	X-VLM	GAP	40.55	37.05	40.9	34.71	95.47	89.53	57	54.94	73.82	70.35	55.26	49.54
		Ours	<b>60.79</b>	<b>71.70</b>	<b>61.53</b>	<b>70.64</b>	<b>99.04</b>	<b>96.07</b>	<b>79.82</b>	<b>81.44</b>	<b>87.5</b>	<b>88.38</b>	<b>76.82</b>	<b>78.35</b>
	CLIP <sub>VIT</sub>	GAP	55.17	45.35	57.28	47.62	53.83	43.35	97.79	96.38	75.04	75.1	54.57	49.08
		Ours	<b>63.11</b>	<b>63.53</b>	<b>63.54</b>	<b>62.21</b>	<b>59.64</b>	<b>58.56</b>	<b>98.97</b>	<b>98.14</b>	<b>81.45</b>	<b>86.91</b>	<b>66.19</b>	<b>68.48</b>
	CLIP <sub>CNN</sub>	GAP	47.62	40.45	49.23	42.83	45.26	39.04	39.57	40.75	91.43	94.47	47.4	43.21
		Ours	<b>51.10</b>	<b>56.63</b>	<b>54.29</b>	<b>59.38</b>	<b>52.84</b>	<b>56.05</b>	<b>64.06</b>	<b>70.25</b>	<b>95.30</b>	<b>94.59</b>	<b>55.74</b>	<b>63.54</b>
	BLIP	GAP	32.37	43.98	35.74	41.59	32.75	29.37	55.7	53.55	67.32	66.98	75.17	73.76
		Ours	<b>46.69</b>	<b>52.86</b>	<b>43.52</b>	<b>50.63</b>	<b>34.92</b>	<b>44.77</b>	<b>70.58</b>	<b>75.81</b>	<b>76.63</b>	<b>81.87</b>	<b>95.84</b>	<b>95.86</b>

**Baselines.** To better reveal the superiority of our proposed method in attacking VLP models, we transplant a typical and powerful algorithm GAP [16] to the multimodal attack scenarios by correspondingly modifying its original loss function. Besides, we also compare with the state-of-the-art (SOTA) instance-specific methods SGA [13] and TMM [14]. To reveal our achieved great black-box transferability. However, it is important to note that universal adversarial attacks usually do not directly compare with the instance-specific methods due to the fairness consideration.

**Implementation details.** Following previous works [13], [14], we adopt the Karpathy split [64] to preprocess the dataset and build the test set for performance evaluation. As for the budget of the perturbation, we follow the previous work [14], limiting the visual perturbation  $\epsilon_v$  to 12/255 and restricting the language perturbation  $\epsilon_t$  to 1 for invisibility. Furthermore, similar to [13], we resize the original images into five scales, i.e.,  $\{0.5, 0.75, 1, 1.25, 1.5\}$ , and add random noise for augmentation.

**Generator Training.** For Flickr30K and MSCOCO, we randomly sample 30,000 images and their captions from the training set to train our perturbation generator. For SNLI-VE and RefCOCO+, we learn our generator directly using their training set with 29,783 and 16,992 images respectively. We initialize the noise variable  $z_v$  as a  $3 \times 3$  matrix. The

dimensions of the initial noise  $z_t$  in the text modality depend on the size of the hidden layer within the specific model. Concretely, we set the noise's dimension to  $1 \times 3$  for ALBEF, TCL, BLIP, and X-VLM, while  $1 \times 2$  for the CLIP model. The generator is trained over 40 epochs with the Adam optimizer, utilizing a learning rate of  $2^{-4}$ .

## 5.2. Attack Effectiveness

In alignment with previous adversarial attacks on VLP models [12], [13], [14], we first consider the typical multimodal task of image-text retrieval and conduct thorough experiments on MSCOCO and Flickr30K to expose the powerful attack effects of the proposed C-PGC. Experimental results on six different VLP models are presented in Table 1. We also provide a visualization example of the image retrieval on the MSCOCO dataset in Figure 4.

**White-box attack performance.** By observing the white-box ASR in the gray-shaded area, we demonstrate that the proposed algorithm achieves excellent attack results on all the evaluated VLP models, validating the outstanding generalization of the produced UAP. With only a single pair of perturbations, we reach a noteworthy average white-box ASR of over 90% on two large datasets in terms of both TR and IR tasks. Especially on the MSCOCO dataset,

TABLE 2. ASR (%) COMPARISON OF OUR METHOD WITH THE SOTA INSTANCE-SPECIFIC METHODS ON ITR TASKS USING THE FLICKR30K DATASET. THE SUBSTITUTE MODEL IS ALBEF AND WE PRESENT THE BLACK-BOX FOOLING RATES ON DIFFERENT TARGET MODELS.

Target model	Method	TR	IR
TCL	SGA	43.95	48.83
	TMM	64.97	<b>69.60</b>
	Ours	<b>66.67</b>	69.59
XVLM	SGA	26.54	39.11
	TMM	<b>47.14</b>	<b>55.49</b>
	Ours	31.40	44.75
CLIP <sub>VIT</sub>	SGA	33.83	43.57
	TMM	52.90	60.90
	Ours	<b>60.84</b>	<b>73.56</b>
CLIP <sub>CNN</sub>	SGA	34.39	46.68
	TMM	56.61	62.97
	Ours	<b>74.22</b>	<b>81.62</b>
BLIP	SGA	39.65	53.65
	TMM	59.99	66.01
	Ours	<b>72.13</b>	<b>73.84</b>

our method achieves over 95% average ASR for both IR and TR tasks across six surrogate models. Compared with the GAP, the proposed method significantly improves the average fooling rates by nearly 10%, which confirms the great validity of our suggested design for universal multimodal attacks. Essentially, the exceptional performance stems from the efficacy of our generated universal perturbations in destroying the alignment between the image and text modalities, thereby misleading the model during inference.

**Black-box attack performance.** We also conduct thorough experiments regarding the attack performance when transferring from surrogate models to other inaccessible models to analyze the adversarial transferability of our algorithm. As demonstrated in Table 1, the proposed C-PGC displays great attack performance in the more realistic black-box scenarios, e.g., 89.24% from TCL to CLIP<sub>CNN</sub> on MSCOCO for IR tasks. We also notice that the advantage of C-PGC over GAP [16] is further amplified by the challenging black-box scenarios, which achieves an average improvement of around 20%. These experimental results indicate that our generative contrastive learning framework does not overly rely on the encoded feature space tailored to the surrogate model. Conversely, it is well capable of transferring to breaking the multimodal alignment of other unseen target models, thus attaining superior attack ability.

To more intuitively show the advantages of our transferability, we also introduce the SOTA instance-specific transferable adversarial attacks SGA [13] and TMM [14] as baselines for comparison. It is noteworthy that our method only employs a single pair of UAP, while SGA and TMM need to generate perturbations for each input image&text pair. Despite the inherent unfairness to our method, C-PGC still brings a notable 5.20% increase in average black-box attack ASR compared to these baselines, as illustrated in Table 2. This again underscores the remarkable adversarial transferability of our method.

### 5.3. Ablation Study

In this part, we utilize the widely adopted ALBEF [1] model as the surrogate to provide ablation studies and in-depth analyses of our attacks. We commence our analysis by examining the contribution of each proposed technique to the generated UAP’s attack ability.

**The effect of  $\mathcal{L}_{CL}$ .** A variant C-PGC<sub>CL</sub>, which removes  $\mathcal{L}_{CL}$  from the training loss of the original method, is first introduced to investigate the impact of the proposed multimodal contrastive loss. As shown in Table 3, the removal of this term results in significant performance degradation, e.g., a 24.74% ASR drop for TR tasks in black-box attack from ALBEF to TCL. This validates the significant contribution of  $\mathcal{L}_{CL}$  to the attack performance and further proves that this loss function can efficiently disrupt the feature alignment to promote a successful attack.

**The effect of  $\mathcal{L}_{dis}$ .** Next, we examine the influence of the unimodal loss  $\mathcal{L}_{dis}$  to the attack effects. C-PGC<sub>dis</sub> is a version of C-PGC where we abandon the  $\mathcal{L}_{dis}$  from the training loss. By comparing the ASRs in Table 3, we demonstrate that this term can further enhance the attack capability on the basis of  $\mathcal{L}_{CL}$ , e.g., a 9.21% increase in the ASR of TR when transferring from ALBEF to the TCL model, proving the importance of the unimodal guidance. These two losses complement each other and jointly underpin the generalizability of the generated perturbations.

**The effect of choice of positive samples.** For the positive samples in the  $\mathcal{L}_{CL}$  loss, we select the data that is farthest from the clean sample within the randomly sampled set. To validate the effectiveness of this farthest sample selection strategy, we introduced a variant called C-PGC<sub>avg</sub> which uses the average embeddings of randomly sampled data as the positive sample. Through experimental results in 3, we reveal that adopting the farthest sample selection approach brings an average improvement of 25.8% and 4.23% for white-box and black-box ASR respectively. Comparing the results of C-PGC<sub>avg</sub> and C-PGC<sub>CL</sub>, we can also conclude that if the positive samples are not adequately defined, adding  $\mathcal{L}_{CL}$  would even cause a negative impact on the white-box attack performance, again verifying the necessity of the proposed farthest samples selection strategy.

**The effect of generator  $G$ .** C-PGC<sub>G</sub> is the version of C-PGC without the perturbation generator, i.e., we directly randomly initialize and update the adversarial perturbation. The results in Table 3 reveal that the absence of the generator’s powerful distribution perception capability results in a pronounced reduction in the generalization capability of the learned UAP on test samples, thereby leading to an obvious decrease in the ASR. Specifically, we find that removing the generator will result in a significant performance drop of more than 50% on average. The generator contributes much more to the final attack performance than all of the remaining loss terms. These findings strongly confirm the crucial importance of introducing the generative network.

**The effect of cross-modal conditions.** To leverage the crucial cross-modal information in multimodal learning, we employ the cross-attention mechanism to allow the generator

TABLE 3. ASR (%) OF C-PGC AND ITS DIFFERENT VARIANTS ON IMAGE-TEXT RETRIEVALS. THE SURROGATE MODEL IS ALBEF AND THE DATASET IS FLICKR30K. THE RESULTS ACROSS SIX TARGET MODELS PROVE THE EFFECTIVENESS OF EACH PROPOSED TECHNIQUE.

Method	ALBEF		TCL		X-VLM		CLIP <sub>ViT</sub>		CLIP <sub>CNN</sub>		BLIP	
	TR	IR	TR	IR	TR	IR	TR	IR	TR	IR	TR	IR
C-PGC	<b>90.24</b>	<b>89.51</b>	<b>66.67</b>	<b>69.59</b>	<b>31.4</b>	<b>44.75</b>	<b>60.84</b>	<b>73.56</b>	<b>74.22</b>	<b>81.62</b>	<b>72.13</b>	<b>73.84</b>
C-PGC <sub>CL</sub>	77.6	78.38	41.93	53.43	17.78	36.24	57.39	70.24	66.84	76.23	51.84	64.96
C-PGC <sub>dis</sub>	80.68	84.13	57.46	67.46	25.07	42.34	58.21	71.52	70.34	79.01	69.34	71.82
C-PGC <sub>avg</sub>	62.8	65.35	53.31	58.93	25.41	40.74	60.56	73.26	73.96	81.58	66.67	71.9
C-PGC <sub>G</sub>	10.2	10.92	4.87	15.47	3.15	12.88	21.31	38.12	24.74	42.12	6.83	18.11
C-PGC <sub>CA</sub>	86.31	87.95	51.86	60.09	20.02	37.62	55.54	68.42	66.97	76.19	60.88	69.89

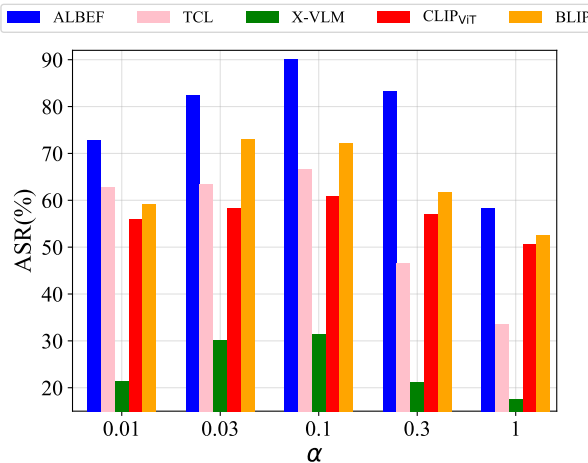


Figure 5. ASR of five target models on the TR task under various values of  $\alpha$ . The surrogate model is ALBEF and the dataset is Flickr30K. Note that when  $\alpha = 0.1$ , the ASR of each target model reaches the top value.

to incorporate cross-modal representations, which helps the generator better destruct the modality alignment. C-PGC<sub>CA</sub> represents a variant where these cross-attention layers are removed. The average 7.22% decrease across six models confirms the vital role of the cross-modal conditions. We can also find that removing cross-modal conditions induces a more pronounced decrease in black-box performance than the white-box attacks, indicating that this technique contributes more to the attack transferability.

Next, we investigate the impact of certain hyperparameters on the overall attack performance.

**Different loss regulation factors  $\alpha$ .** The value of  $\alpha$  is a critical factor for the attack effects as it adjusts the scales of the two important loss terms  $\mathcal{L}_{CL}$  and  $\mathcal{L}_{dis}$ . We then explore the attack performance corresponding to different values of  $\alpha$ , including 0.01, 0.03, 0.1, 0.3, and 1, to confirm the optimal parameter setting. The results in Figure 5 indicate that when  $\alpha$  is set to 0.1, our method achieves significantly superior performance.

**Different image perturbation budget  $\epsilon_v$ .** The magnitude of image perturbations is a crucial metric for adversarial attacks. As shown in Figure 6, we tested the attack performance under varying perturbation magnitudes ranging from 4/255 to 16/255. It can be observed that the overall

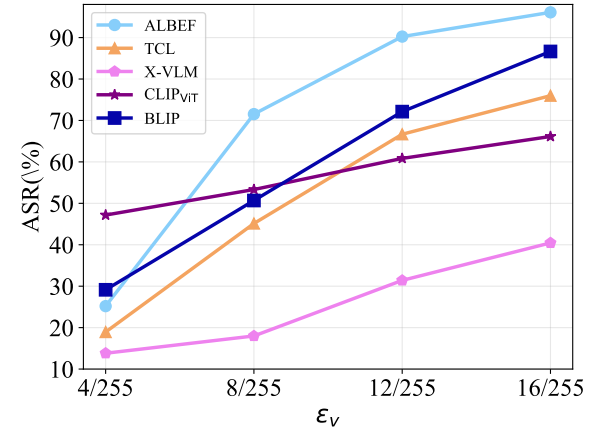


Figure 6. ASR of five target models on the TR task under various values of  $\epsilon_v$ . The surrogate model is ALBEF and the dataset is Flickr30K. As the budget  $\epsilon_v$  increases, the ASR of each target model is also getting higher.

attack performance increases with the larger perturbation magnitudes both for the white-box and black-box settings. Note that when the perturbation magnitude is 4/255, C-PGC's attack performance is severely compromised. The underlying reason is that with only one common perturbation, the budget 4/255 is too small to allow the generated UAP to carry enough information that is required to generalize to different data samples. We also noticed that from 12/255 to 16/255, the degree of improvement brought by increasing the perturbation budget slows down. Therefore, we selected a moderate perturbation range of 12/255 to reach a balance between attack utility and imperceptibility.

**Different text perturbation budget  $\epsilon_t$ .** We also evaluate the attack effects under different values of the text perturbation budget  $\epsilon_t$ , including 1, 2, 3, and 4. Due to the page limit, the detailed results and analysis are presented in Fig 8 of Appendix D.

#### 5.4. Evaluation on More Scenarios

To further reveal the effectiveness of the proposed algorithm, we consider a range of scenarios including more downstream V+L tasks, cross-domain transfer, and attacking the cutting-edge large vision-language models (LVLMs).

**More downstream tasks.** The cross-modal interactions and alignment play an important part in multimodal learning regardless of the downstream tasks. We prove that the proposed method is capable of effectively destroying the alignment relationship by presenting results on more V+L tasks. Specifically, we further discuss and evaluate C-PGC on Image Captioning (IC), Visual Grounding (VG), and Visual Entailment (VE). Note that the results of VE are shown in Appendix B.

TABLE 4. PERFORMANCE OF IMAGE CAPTIONING. THE BASELINE REPRESENTS THE ORIGINAL PERFORMANCE OF THE TARGET MODEL ON CLEAN DATA. THE TARGET MODEL IS BLIP.

Source	B@4	METEOR	ROUBE_L	CIDEr	SPICE
Baseline	38.8	29.9	59.4	133.1	23
ALBEF	34.5	26.7	57.2	124.4	21.8
TCL	34.7	26.9	57.6	122.3	21.9
BLIP	<b>33.4</b>	<b>25.7</b>	<b>56.8</b>	<b>119.1</b>	<b>20.8</b>

**Image captioning.** The objective of this task is to encode an input image into image embeddings and subsequently utilize an image-conditioned language modeling module to generate text descriptions relevant to the image content based on the encoded image representations. We use ALBEF, TCL, and BLIP as source models and directly attack the commonly used captioning model BLIP with the MSCOCO dataset. Similarly to SGA [13], several typical and commonly used metrics are calculated to evaluate the quality of the generated captions, including BLEU [65], METEOR [66], ROUGE [67], CIDEr [68], and SPICE [69]. The results presented in Table 4 demonstrate that our algorithm displays prominent attack effects against the image captioning task. For instance, when transferred from ALBEF to BLIP, the crafted UAP induces notable drops of 11% and 10.7% in the B@4 and METEOR metrics, respectively.

**Visual grounding.** This is another commonly considered V+L task, which aims to locate the corresponding position in an image based on a given textual description. We conduct experiments on RefCOCO+ [63] dataset using ALBEF, TCL, and X-VLM both as source and target models. As shown in Table 5, the results indicate that our attack brings remarkable negative effects on the localization accuracy for both white-box and black-box settings, again verifying that the produced UAP strongly breaks the cross-modal interaction and alignment.

**Cross-domain scenarios.** We proceed to discuss the attack performance of the proposed algorithm in a more challenging scenario where an obvious distribution shift exists between the training and testing data. Specifically, we generate universal adversarial perturbations on MSCOCO or Flickr30 and evaluate them accordingly on another dataset. We present the attack success rates transfer from MSCOCO to Flickr30 on the retrieval tasks in Table 7. It can be observed that the domain gap only brings a limited decrease to the proposed attack, unveiling the outstanding cross-domain transferability of the C-PGC. For attack results from Flickr30 to MSCOCO, please refer to Appendix D.

TABLE 5. PERFORMANCE OF VISUAL GROUNDING. THE BASELINE INDICATES THE ORIGINAL PERFORMANCE OF THE TARGET MODEL ON CLEAN DATA.

Source	Target	Val	TestA	TestB
Baseline	ALBEF	58.4	65.9	46.2
ALBEF		<b>43.1</b>	<b>39.0</b>	<b>32.0</b>
TCL		47.2	46.7	35.2
X-VLM		44.1	39.3	32.9
Baseline	TCL	59.6	66.8	48.1
ALBEF		53.9	47.9	37.1
TCL		<b>42.1</b>	<b>41.3</b>	<b>33.3</b>
X-VLM		42.5	41.8	34.2
Baseline	X-VLM	47.6	53.8	42.2
ALBEF		40.3	43.1	35.9
TCL		38.6	43.5	35.7
X-VLM		<b>34.3</b>	<b>37.7</b>	<b>32.9</b>

TABLE 6. ASR (%) ON DIFFERENT LVLMs. WE ADOPT THE THREE DIFFERENT SOURCE MODELS AND LAUNCH TRANSFERABLE ATTACKS TO THE LVLMs.

Target model	Source model		
	ALBEF	TCL	BLIP
Qwen-VL	13.72	9.56	6.40
VisualGLM	14.22	18.54	16.67
LLaVA-7B	7.82	8.50	8.20
LLaVA-13B	33.88	19.61	19.17
MiniGPT-4_7B	70.50	68.68	69.87
MiniGPT-4_13B	24.59	20.69	25.92

**Transfer to LVLMs.** Recently, large general models capable of handling complex vision-language tasks have been rapidly developing and attracting widespread attention.

To further demonstrate the potential threat posed by our method in more practical scenarios, we intend to evaluate C-PGC’s performance on multiple mainstream LVLMs, including the powerful LLaVA [21], Qwen-VL [20], Mini-GPT4 [70], and VisualGLM [71]. Given the immense number of parameters of these large models, it is infeasible for users to train and use them locally [14]. Consequently, we consider more practical transfer attacks to assess the threat posed by our method to LVLMs.

Similar to the test protocol in TMM [14], we make queries to ask the large models to determine whether the adversarial image corresponds to the adversarial text. We craft adversarial samples with images from the Flickr30k dataset and present the results in Table 6. It demonstrates that the proposed method achieves impressive transferability to deceive the LVLMs. Especially on the widely used MiniGPT-4\_7B, the produced UAP can even achieve nearly 70% ASR. We also find that an LVLM with better language comprehension and generation ability (e.g., LLaVA and Qwen-VL) exhibits better robustness against adversarial attacks. Additionally, the model architecture and the number of parameters in the LVLM also have a notable impact on the

TABLE 7. ASR (%) OF CROSS-DOMAIN ATTACKS FROM MSCOCO TO FLICKR30. THE GRAY SHADING INDICATES WHITE-BOX ATTACKS.

Source	ALBEF		TCL		X-VLM		CLIP <sub>ViT</sub>		CLIP <sub>CNN</sub>		BLIP	
	TR	IR	TR	IR	TR	IR	TR	IR	TR	IR	TR	IR
ALBEF	<b>88.59</b>	<b>87.95</b>	60.87	66.36	23.07	40.25	57.88	69.00	69.04	76.02	62.99	67.09
TCL	55.40	60.69	<b>88.72</b>	<b>85.09</b>	24.70	41.00	67.24	77.48	75.26	82.77	66.04	71.05
X-VLM	35.77	54.33	38.3	56.14	<b>81.1</b>	<b>82.24</b>	64.16	71.45	75.52	80.39	58.78	68.69
CLIP <sub>ViT</sub>	37.31	49.62	45.86	54.40	32.00	46.62	<b>84.33</b>	<b>86.22</b>	64.12	77.1	43.74	57.69
CLIP <sub>CNN</sub>	29.29	46.32	36.02	51.52	27.24	45.97	41.75	63.06	<b>82.34</b>	<b>88.47</b>	36.8.	55.34
BLIP	39.83	41.77	37.36	44.20	23.58	35.31	54.68	68.77	65.41	75.00	<b>86.96</b>	<b>89.80</b>

TABLE 8. ASR (%) OF ITR TASKS UNDER DIFFERENT DEFENSE STRATEGIES. THE SURROGATE MODEL IS ALBEF AND THE DATASET IS FLICK30K. THE LT DENOTES THE LANGUAGETOOL THAT CORRECTS ADVERSARIAL WORDS WITHIN THE SENTENCE.

Method	ALBEF		TCL		X-VLM		CLIP <sub>ViT</sub>		CLIP <sub>CNN</sub>		BLIP	
	TR	IR	TR	IR	TR	IR	TR	IR	TR	IR	TR	IR
Gaussian	58.75	59.98	34.99	48.71	19.82	39.13	52.46	<b>68.20</b>	64.90	78.40	43.53	57.12
Medium	64.78	65.09	47.00	57.38	26.73	44.66	59.24	72.66	73.83	82.18	57.31	65.91
Average	51.35	55.34	32.51	47.55	18.6	37.49	51.97	68.55	65.67	78.57	44.37	58.4
JPEG	71.53	70.86	57.14	62.16	45.73	55.62	59.48	74.93	72.02	81.79	63.93	72.83
DiffPure	64.03	74.23	65.73	74.49	64.23	74.63	77.96	86.25	81.12	87.39	69.51	78.93
NRP	32.23	40.81	<b>22.05</b>	<b>41.16</b>	15.85	33.79	53.33	69.54	61.53	<b>76.86</b>	37.43	<b>53.17</b>
NRP+LT	<b>29.62</b>	<b>35.27</b>	24.02	45.16	<b>13.03</b>	<b>30.69</b>	<b>51.39</b>	69.23	<b>60.21</b>	77.51	<b>36.49</b>	57.17

attack effects and the effect depends on the specific model type. For instance, LLaVA-7B exhibits a higher robustness than its 13B version while MiniGPT-4\_13B is significantly more robust than its 7B version.

## 6. Defense Strategies

To mitigate the potential harm brought by the proposed attack, we evaluate several defense strategies to explore possible defense methods against the C-PGC.

To deal with adversarial attacks, adversarial training appears to be a highly reliable defense mechanism that can essentially enhance the robustness of victim models. Extensive research has explored adversarial training for VLP models [72], [73] and achieved remarkable adversarial robustness. However, adversarial training for VLP models requires huge computational costs and time. Therefore, we align with TMM [14] and consider some universal defense strategies that are not tailored to specific models. Specifically, we discuss several input preprocessing-based schemes, including image smoothing [74] (Gaussian, medium, average smoothing), JPEG compression [75], NRP [76], and the recently prevalent DiffPure [77], a powerful purification defense based on diffusion models. For text preprocessing, we choose the LanguageTool (LT) employed in [14] for adversarial text correction, which has been widely adopted in various scenarios due to its universality and effectiveness. Attack results using ALBEF as the substitute model in Table 8 demonstrate that the proposed attack still attains great performance in most cases. NRP+LT would be a good choice to alleviate the threat brought by C-PGC. Besides,

although the DiffPure [77] effectively defends previous attacks in classification tasks, their ability is largely reduced in V+L scenarios since their denoise process also diminishes some texture or semantic information that is critical in VLP models, thereby acquiring unsatisfactory defense results.

## 7. Related Works

### 7.1. Adversarial Learning

**Adversarial Attacks.** Among various attacks and defenses on DNNs [78], [79], [80], [81], [82], the adversarial attack is the most appealing one which applies well-designed modifications in the forms of perturbations [7], [8], [83], [84], [85] or patches [86], [87], [88] to the input samples. Based on the adversary’s knowledge about the target model, adversarial attacks can be divided into white-box attacks [7], [8], [89], [90], [91], [92] and black-box attacks [93], [94], [95], [96]. In white-box settings, most adversarial attacks leverage the gradients of the fully accessible target model to generate adversarial examples, such as FGSM [8], PGD [92], C&W [7], DeepFool [91], JSMA [90], and MIM [89]. But in black-box settings, the architectures and parameters become unavailable. Thus, black-box adversarial attacks are conducted by leveraging the output of the victim model [95], [96] (i.e., query-based attacks), or generating adversarial examples based on the surrogate model [93], [94] (i.e., transfer-based methods). Transfer-based black-box attacks further introduce the concept of adversarial transferability, which measures to what extent the adversarial samples generated by the surrogate model generalize to the

unknown target model. Besides, the discrete nature of texts can be a great challenge when applying adversarial attacks to NLP tasks. Therefore, existing adversarial attacks in NLP primarily focus on how to alter some tokens of the original texts to increase the probabilities of embedding errors [97], [98], [99], [100].

**Adversarial Defenses.** Adversarial training [8], [101], [102], [103] is one effective solution to defend adversarial attacks, which integrates both benign samples and adversarial samples into the training process to increase adversarial robustness. However, it is difficult to incorporate all kinds of possible adversarial samples during adversarial training and as a result, this defense strategy may not generalize well to unseen attacks. Besides, adversarial training is often computationally expensive in practical scenarios. Hence, to address this problem, some other defense methods [104], [105], [106], [107] propose to apply different pre-processing procedures and transformations on the input samples, or [108], [109] carefully design new objective functions to promote the compactness of representations. Commonly used pre-processing techniques include image smoothing [74], JPEG compression [75], NRP [76], and DiffPure [77]. As for the defenses in NLP tasks, current methods come into effect by passively detecting the adversarial samples during the inference time [110], [111] or proactively improving the robustness during the training time [112], [113].

## 7.2. Universal Adversarial Examples

Universal adversarial attacks [15], [114], [115], [116], [117], [118] aim to deceive the victim model by exerting a unified adversarial modification on all the benign samples. By adopting the paradigm of attacking all the clean samples with one uniform modification, these attacks save the redundant procedures of redesigning adversarial modifications for each input and are consequently more efficient than conventional adversarial attacks. Most universal adversarial attacks can be categorized into optimization-based methods [15], [114], [115] and generation-based methods [116], [117], [118]. Benefiting from the powerful learning abilities of generative models, generation-based methods are more versatile and can produce more natural samples when compared with optimization-based methods. However, a majority of previous generation-based methods are only restricted to single-model attacks and rely heavily on the label information of the target model, which is likely to be unavailable in realistic scenarios. To fill this gap, Zhou *et al.* [119] propose to exploit the high-frequency components and design a downstream-agnostic generative universal attack framework, which significantly improves the attack success rates based on the pre-trained encoder. In this paper, we manage to generate universal adversarial examples for VLP models with high attack success rates.

## 8. Limitations of the Attack

**Overlook of interactions between perturbations  $\delta_v$  and  $\delta_t$ .** The proposed framework generates universal per-

turbations for image and text respectively based on the designed multimodal and unimodal losses. Despite the remarkable attack performance, it does not take into account the interactions and synergy between the perturbations  $\delta_v$  and  $\delta_t$ , which has been leveraged in several previous attacks [13], [14] for improved performance. In future research, we can consider utilizing this potential mechanism to further boost our attacks.

**Textual Semantic Inconsistency.** To ensure the stealthiness of textual attacks, we set the perturbation budget  $\epsilon_t = 1$ , which indicates that only one word is modified. Nonetheless, this perturbation is still relatively likely to be detected since it is considerably difficult to maintain semantic consistency between the clean and the perturbed sentences when applying one universal word to various attacked texts. For instance, when the adversarial word is *getting* (verb) and the word to replace is *bed* (noun), the resultant adversarial text becomes *A getting is unmade with pillows on it*, which is somehow strange and highly likely to attract the attention of defense systems or humans. This is an inevitable common issue for the whole textual UAP field. A possible solution is to add perturbations to the word embeddings instead of the sentence. However, this only applies to white-box scenarios given that black-box scenarios require sentences as input and attackers have no access to the word embeddings. Furthermore, the dimensions of word embedding also vary across different VLP models.

## 9. Conclusion

This paper delves into the challenging task of launching universal adversarial attacks against VLP models and proposes an effective solution that achieves superior attack performance using only one universal pair of image-text perturbations. We begin by revealing the considerably unsatisfactory results of existing UAP methods and empirically explaining the underlying reasons. Based on our analysis, we propose to break the crucial cross-modal alignment in VLP models by designing a contrastive-learning generative UAP framework, which leverages both unimodal and multimodal information to enhance the attacks. Extensive experiments validate the efficacy of the proposed algorithm on diverse VLP models and V+L tasks. Particularly, the performance under black-box settings demonstrates that our method exhibits excellent adversarial transferability, surpassing the SOTA instance-specific transferable attacks [13], [14]. Moreover, we evaluate C-PGC when transferred to multiple prevalent LLVMs and show that it achieves an impressive attack success rate. Additionally, the decent attack performance under 8 mainstream defense strategies renders C-PGC a more formidable threat. We highlight the proposed attack is of significant practicality and applicability, which can serve as a reliable tool to analyze the adversarial robustness of different VLP models. We also hope that this paper can promote future research that further explores more sophisticated defenses to strengthen the resilience of VLP models against adversarial attacks.

## References

[1] J. Li, R. Selvaraju, A. Gotmare, S. Joty, C. Xiong, and S. C. H. Hoi, “Align before fuse: Vision and language representation learning with momentum distillation,” *Advances in Neural Information Processing Systems*, vol. 34, pp. 9694–9705, 2021.

[2] J. Yang, J. Duan, S. Tran, Y. Xu, S. Chanda, L. Chen, B. Zeng, T. Chilimbi, and J. Huang, “Vision-language pre-training with triple contrastive learning,” in *CVPR*, 2022, pp. 15 671–15 680.

[3] H. Song, L. Dong, W.-N. Zhang, T. Liu, and F. Wei, “Clip models are few-shot learners: Empirical studies on vqa and visual entailment,” *arXiv preprint arXiv:2203.07190*, 2022.

[4] K. Wang, Q. Yin, W. Wang, S. Wu, and L. Wang, “A comprehensive survey on cross-modal retrieval,” *arXiv preprint arXiv:1607.06215*, 2016.

[5] R. Hong, D. Liu, X. Mo, X. He, and H. Zhang, “Learning to compose and reason with language tree structures for visual grounding,” *IEEE transactions on pattern analysis and machine intelligence*, vol. 44, no. 2, pp. 684–696, 2019.

[6] N. Xie, F. Lai, D. Doran, and A. Kadav, “Visual entailment: A novel task for fine-grained image understanding,” *arXiv preprint arXiv:1901.06706*, 2019.

[7] N. Carlini and D. Wagner, “Towards evaluating the robustness of neural networks,” in *2017 ieee symposium on security and privacy (sp)*. Ieee, 2017, pp. 39–57.

[8] I. J. Goodfellow, J. Shlens, and C. Szegedy, “Explaining and harnessing adversarial examples,” *arXiv preprint arXiv:1412.6572*, 2014.

[9] K. Eykholt, I. Evtimov, E. Fernandes, B. Li, A. Rahmati, C. Xiao, A. Prakash, T. Kohno, and D. Song, “Robust physical-world attacks on deep learning visual classification,” in *CVPR*, 2018, pp. 1625–1634.

[10] S. K. Sarkar, K. Oshiba, D. Giebisch, and Y. Singer, “Robust classification of financial risk,” *arXiv preprint arXiv:1811.11079*, 2018.

[11] X. Yang, Y. Dong, T. Pang, H. Su, J. Zhu, Y. Chen, and H. Xue, “Towards face encryption by generating adversarial identity masks,” in *ICCV*, 2021, pp. 3897–3907.

[12] J. Zhang, Q. Yi, and J. Sang, “Towards adversarial attack on vision-language pre-training models,” in *Proceedings of the 30th ACM International Conference on Multimedia*, 2022, pp. 5005–5013.

[13] D. Lu, Z. Wang, T. Wang, W. Guan, H. Gao, and F. Zheng, “Set-level guidance attack: Boosting adversarial transferability of vision-language pre-training models,” in *ICCV*, 2023, pp. 102–111.

[14] H. Wang, K. Dong, Z. Zhu, H. Qin, A. Liu, X. Fang, J. Wang, and X. Liu, “Transferable multimodal attack on vision-language pre-training models,” in *2024 IEEE Symposium on Security and Privacy (SP)*. IEEE Computer Society, 2024, pp. 102–102.

[15] S.-M. Moosavi-Dezfooli, A. Fawzi, O. Fawzi, and P. Frossard, “Universal adversarial perturbations,” in *CVPR*, 2017, pp. 1765–1773.

[16] O. Poursaeed, I. Katsman, B. Gao, and S. Belongie, “Generative adversarial perturbations,” in *CVPR*, 2018, pp. 4422–4431.

[17] X. Liu, Y. Zhong, Y. Zhang, L. Qin, and W. Deng, “Enhancing generalization of universal adversarial perturbation through gradient aggregation,” in *ICCV*, 2023, pp. 4435–4444.

[18] J. Li, D. Li, C. Xiong, and S. Hoi, “Blip: Bootstrapping language-image pre-training for unified vision-language understanding and generation,” in *ICML*. PMLR, 2022, pp. 12 888–12 900.

[19] A. S. Hashemi, A. Bär, S. Mozaffari, and T. Fingscheidt, “Transferable universal adversarial perturbations using generative models,” *arXiv preprint arXiv:2010.14919*, 2020.

[20] J. Bai, S. Bai, S. Yang, S. Wang, S. Tan, P. Wang, J. Lin, C. Zhou, and J. Zhou, “Qwen-vl: A frontier large vision-language model with versatile abilities,” *arXiv preprint arXiv:2308.12966*, 2023.

[21] H. Liu, C. Li, Q. Wu, and Y. J. Lee, “Visual instruction tuning,” *NeurIPS*, vol. 36, 2024.

[22] F.-L. Chen, D.-Z. Zhang, M.-L. Han, X.-Y. Chen, J. Shi, S. Xu, and B. Xu, “Vlp: A survey on vision-language pre-training,” *Machine Intelligence Research*, vol. 20, no. 1, pp. 38–56, 2023.

[23] Y. Du, Z. Liu, J. Li, and W. X. Zhao, “A survey of vision-language pre-trained models,” *arXiv preprint arXiv:2202.10936*, 2022.

[24] J. D. M.-W. C. Kenton and L. K. Toutanova, “Bert: Pre-training of deep bidirectional transformers for language understanding,” in *Proceedings of NAACL-HLT*, 2019, pp. 4171–4186.

[25] L. H. Li, M. Yatskar, D. Yin, C.-J. Hsieh, and K.-W. Chang, “Visu-albert: A simple and performant baseline for vision and language,” *arXiv preprint arXiv:1908.03557*, 2019.

[26] P. Zhang, X. Li, X. Hu, J. Yang, L. Zhang, L. Wang, Y. Choi, and J. Gao, “Vinvl: Revisiting visual representations in vision-language models,” in *CVPR*, 2021, pp. 5579–5588.

[27] Y. Zeng, X. Zhang, and H. Li, “Multi-grained vision language pre-training: Aligning texts with visual concepts,” in *ICML*. PMLR, 2022, pp. 25 994–26 009.

[28] J. Lu, D. Batra, D. Parikh, and S. Lee, “Vilbert: Pretraining task-agnostic visiolinguistic representations for vision-and-language tasks,” *NeurIPS*, vol. 32, 2019.

[29] X. Li, X. Yin, C. Li, P. Zhang, X. Hu, L. Zhang, L. Wang, H. Hu, L. Dong, F. Wei *et al.*, “Oscar: Object-semantics aligned pre-training for vision-language tasks,” in *Computer Vision–ECCV 2020: 16th European Conference, Glasgow, UK, August 23–28, 2020, Proceedings, Part XXX 16*. Springer, 2020, pp. 121–137.

[30] G. Li, N. Duan, Y. Fang, M. Gong, and D. Jiang, “Unicodervl: A universal encoder for vision and language by cross-modal pre-training,” in *Proceedings of the AAAI conference on artificial intelligence*, vol. 34, no. 07, 2020, pp. 11 336–11 344.

[31] Z. Wang, J. Yu, A. W. Yu, Z. Dai, Y. Tsvetkov, and Y. Cao, “Simvlm: Simple visual language model pretraining with weak supervision,” in *International Conference on Learning Representations*, 2021.

[32] A. Dosovitskiy, L. Beyer, A. Kolesnikov, D. Weissenborn, X. Zhai, T. Unterthiner, M. Dehghani, M. Minderer, G. Heigold, S. Gelly *et al.*, “An image is worth 16x16 words: Transformers for image recognition at scale,” in *International Conference on Learning Representations*, 2020.

[33] A. Radford, J. W. Kim, C. Hallacy, A. Ramesh, G. Goh, S. Agarwal, G. Sastry, A. Askell, P. Mishkin, J. Clark *et al.*, “Learning transferable visual models from natural language supervision,” in *ICML*. PMLR, 2021, pp. 8748–8763.

[34] Y.-C. Chen, L. Li, L. Yu, A. El Kholy, F. Ahmed, Z. Gan, Y. Cheng, and J. Liu, “Uniter: Universal image-text representation learning,” in *ECCV*. Springer, 2020, pp. 104–120.

[35] L. Zhou, H. Palangi, L. Zhang, H. Hu, J. Corso, and J. Gao, “Unified vision-language pre-training for image captioning and vqa,” in *Proceedings of the AAAI conference on artificial intelligence*, vol. 34, no. 07, 2020, pp. 13 041–13 049.

[36] S. Zhang, T. Jiang, T. Wang, K. Kuang, Z. Zhao, J. Zhu, J. Yu, H. Yang, and F. Wu, “Devlbert: Learning deconfounded visiolinguistic representations,” in *Proceedings of the 28th ACM International Conference on Multimedia*, 2020, pp. 4373–4382.

[37] Z.-Y. Dou, Y. Xu, Z. Gan, J. Wang, S. Wang, L. Wang, C. Zhu, P. Zhang, L. Yuan, N. Peng *et al.*, “An empirical study of training end-to-end vision-and-language transformers,” in *CVPR*, 2022, pp. 18 166–18 176.

[38] W. Kim, B. Son, and I. Kim, “Vilt: Vision-and-language transformer without convolution or region supervision,” in *ICML*. PMLR, 2021, pp. 5583–5594.

[39] J. Lin, A. Yang, Y. Zhang, J. Liu, J. Zhou, and H. Yang, “Interbert: Vision-and-language interaction for multi-modal pretraining,” *arXiv preprint arXiv:2003.13198*, 2020.

[40] H. Tan and M. Bansal, “Lxmert: Learning cross-modality encoder representations from transformers,” in *Proceedings of the 2019 Conference on Empirical Methods in Natural Language Processing and the 9th International Joint Conference on Natural Language Processing (EMNLP-IJCNLP)*, 2019, pp. 5100–5111.

[41] W. Li, C. Gao, G. Niu, X. Xiao, H. Liu, J. Liu, H. Wu, and H. Wang, “Unimo: Towards unified-modal understanding and generation via cross-modal contrastive learning,” in *Proceedings of the 59th Annual Meeting of the Association for Computational Linguistics and the 11th International Joint Conference on Natural Language Processing (Volume 1: Long Papers)*, 2021, pp. 2592–2607.

[42] H. Xue, Y. Huang, B. Liu, H. Peng, J. Fu, H. Li, and J. Luo, “Probing inter-modality: Visual parsing with self-attention for vision-and-language pre-training,” *NeurIPS*, vol. 34, pp. 4514–4528, 2021.

[43] Z. Huang, Z. Zeng, Y. Huang, B. Liu, D. Fu, and J. Fu, “Seeing out of the box: End-to-end pre-training for vision-language representation learning,” in *CVPR*, 2021, pp. 12976–12985.

[44] C. Jia, Y. Yang, Y. Xia, Y.-T. Chen, Z. Parekh, H. Pham, Q. Le, Y.-H. Sung, Z. Li, and T. Duerig, “Scaling up visual and vision-language representation learning with noisy text supervision,” in *ICML*. PMLR, 2021, pp. 4904–4916.

[45] P. Anderson, X. He, C. Buehler, D. Teney, M. Johnson, S. Gould, and L. Zhang, “Bottom-up and top-down attention for image captioning and visual question answering,” in *CVPR*, 2018, pp. 6077–6086.

[46] Q. Xia, H. Huang, N. Duan, D. Zhang, L. Ji, Z. Sui, E. Cui, T. Bharti, and M. Zhou, “Xgpt: Cross-modal generative pre-training for image captioning,” in *Natural Language Processing and Chinese Computing: 10th CCF International Conference, NLPCC 2021, Qingdao, China, October 13–17, 2021, Proceedings, Part I 10*. Springer, 2021, pp. 786–797.

[47] A. Kamath, M. Singh, Y. LeCun, G. Synnaeve, I. Misra, and N. Carion, “Mdetr-modulated detection for end-to-end multi-modal understanding,” in *ICCV*, 2021, pp. 1780–1790.

[48] P. Kaur, H. S. Pannu, and A. K. Malhi, “Comparative analysis on cross-modal information retrieval: A review,” *Computer Science Review*, vol. 39, p. 100336, 2021.

[49] L. Ying, G. Yingying, F. Jie, F. Jiulun, H. Yu, and L. Jiming, “Survey of research on deep learning image-text cross-modal retrieval,” *Journal of Frontiers of Computer Science & Technology*, vol. 16, no. 3, 2022.

[50] S. Bai and S. An, “A survey on automatic image caption generation,” *Neurocomputing*, vol. 311, pp. 291–304, 2018.

[51] H. Wang, Y. Zhang, and X. Yu, “An overview of image caption generation methods,” *Computational intelligence and neuroscience*, vol. 2020, 2020.

[52] O. Vinyals, A. Toshev, S. Bengio, and D. Erhan, “Show and tell: A neural image caption generator,” in *CVPR*, 2015, pp. 3156–3164.

[53] Y. Li, T. Lin, K. Yi, D. Bear, D. Yamins, J. Wu, J. Tenenbaum, and A. Torralba, “Visual grounding of learned physical models,” in *ICML*. PMLR, 2020, pp. 5927–5936.

[54] R. Shrestha, K. Kafle, and C. Kanan, “A negative case analysis of visual grounding methods for vqa,” in *Annual Conference of the Association for Computational Linguistics (ACL)*, 2020.

[55] C. Thomas, Y. Zhang, and S.-F. Chang, “Fine-grained visual entailment,” in *ECCV*. Springer, 2022, pp. 398–416.

[56] T. Kim and J. Ghosh, “On single source robustness in deep fusion models,” *Advances in Neural Information Processing Systems*, vol. 32, 2019.

[57] M. Shah, X. Chen, M. Rohrbach, and D. Parikh, “Cycle-consistency for robust visual question answering,” in *CVPR*, 2019, pp. 6649–6658.

[58] K. Yang, W.-Y. Lin, M. Barman, F. Condessa, and Z. Kolter, “Defending multimodal fusion models against single-source adversaries,” in *CVPR*, 2021, pp. 3340–3349.

[59] X. Xu, X. Chen, C. Liu, A. Rohrbach, T. Darrell, and D. Song, “Fooling vision and language models despite localization and attention mechanism,” in *CVPR*, 2018, pp. 4951–4961.

[60] K. He, H. Fan, Y. Wu, S. Xie, and R. Girshick, “Momentum contrast for unsupervised visual representation learning,” in *CVPR*, 2020, pp. 9729–9738.

[61] B. A. Plummer, L. Wang, C. M. Cervantes, J. C. Caicedo, J. Hockenmaier, and S. Lazebnik, “Flickr30k entities: Collecting region-to-phrase correspondences for richer image-to-sentence models,” in *ICCV*, 2015, pp. 2641–2649.

[62] T.-Y. Lin, M. Maire, S. Belongie, J. Hays, P. Perona, D. Ramanan, P. Dollár, and C. L. Zitnick, “Microsoft coco: Common objects in context,” in *Computer Vision–ECCV 2014: 13th European Conference, Zurich, Switzerland, September 6–12, 2014, Proceedings, Part V 13*. Springer, 2014, pp. 740–755.

[63] L. Yu, P. Poirson, S. Yang, A. C. Berg, and T. L. Berg, “Modeling context in referring expressions,” in *Computer Vision–ECCV 2016: 14th European Conference, Amsterdam, The Netherlands, October 11–14, 2016, Proceedings, Part II 14*. Springer, 2016, pp. 69–85.

[64] A. Karpathy and L. Fei-Fei, “Deep visual-semantic alignments for generating image descriptions,” in *CVPR*, 2015, pp. 3128–3137.

[65] K. Papineni, S. Roukos, T. Ward, and W.-J. Zhu, “Bleu: a method for automatic evaluation of machine translation,” in *Proceedings of the 40th annual meeting of the Association for Computational Linguistics*, 2002, pp. 311–318.

[66] S. Banerjee and A. Lavie, “Meteor: An automatic metric for mt evaluation with improved correlation with human judgments,” in *Proceedings of the acl workshop on intrinsic and extrinsic evaluation measures for machine translation and/or summarization*, 2005, pp. 65–72.

[67] C.-Y. Lin, “Rouge: A package for automatic evaluation of summaries,” in *Text summarization branches out*, 2004, pp. 74–81.

[68] R. Vedantam, C. Lawrence Zitnick, and D. Parikh, “Cider: Consensus-based image description evaluation,” in *CVPR*, 2015, pp. 4566–4575.

[69] P. Anderson, B. Fernando, M. Johnson, and S. Gould, “Spice: Semantic propositional image caption evaluation,” in *Computer Vision–ECCV 2016: 14th European Conference, Amsterdam, The Netherlands, October 11–14, 2016, Proceedings, Part V 14*. Springer, 2016, pp. 382–398.

[70] D. Zhu, J. Chen, X. Shen, X. Li, and M. Elhoseiny, “Minigpt-4: Enhancing vision-language understanding with advanced large language models,” *arXiv preprint arXiv:2304.10592*, 2023.

[71] Z. Du, Y. Qian, X. Liu, M. Ding, J. Qiu, Z. Yang, and J. Tang, “Glm: General language model pretraining with autoregressive blank infilling,” *arXiv preprint arXiv:2103.10360*, 2021.

[72] Z. Gan, Y.-C. Chen, L. Li, C. Zhu, Y. Cheng, and J. Liu, “Large-scale adversarial training for vision-and-language representation learning,” *NeurIPS*, vol. 33, pp. 6616–6628, 2020.

[73] W. Yang and B. Mirzasoleiman, “Robust contrastive language-image pretraining against adversarial attacks,” *arXiv preprint arXiv:2303.06854*, 2023.

[74] G. W. Ding, L. Wang, and X. Jin, “Advertorch v0. 1: An adversarial robustness toolbox based on pytorch,” *arXiv preprint arXiv:1902.07623*, 2019.

[75] G. K. Dziugaite, Z. Ghahramani, and D. M. Roy, “A study of the effect of jpg compression on adversarial images,” *arXiv preprint arXiv:1608.00853*, 2016.

[76] M. Naseer, S. Khan, M. Hayat, F. S. Khan, and F. Porikli, “A self-supervised approach for adversarial robustness,” in *CVPR*, 2020, pp. 262–271.

[77] W. Nie, B. Guo, Y. Huang, C. Xiao, A. Vahdat, and A. Anandkumar, “Diffusion models for adversarial purification,” *arXiv preprint arXiv:2205.07460*, 2022.

[78] W. Yu, H. Fang, B. Chen, X. Sui, C. Chen, H. Wu, S.-T. Xia, and K. Xu, “Gi-nas: Boosting gradient inversion attacks through adaptive neural architecture search,” *arXiv preprint arXiv:2405.20725*, 2024.

[79] H. Fang, B. Chen, X. Wang, Z. Wang, and S.-T. Xia, “Gifd: A generative gradient inversion method with feature domain optimization,” in *Proceedings of the IEEE/CVF International Conference on Computer Vision*, 2023, pp. 4967–4976.

[80] H. Fang, Y. Qiu, H. Yu, W. Yu, J. Kong, B. Chong, B. Chen, X. Wang, and S.-T. Xia, “Privacy leakage on dnns: A survey of model inversion attacks and defenses,” *arXiv preprint arXiv:2402.04013*, 2024.

[81] K. Gao, Y. Bai, J. Gu, Y. Yang, and S.-T. Xia, “Backdoor defense via adaptively splitting poisoned dataset,” in *CVPR*, 2023, pp. 4005–4014.

[82] K. Gao, J. Bai, B. Wu, M. Ya, and S.-T. Xia, “Imperceptible and robust backdoor attack in 3d point cloud,” *TIFS*, vol. 19, pp. 1267–1282, 2023.

[83] S. Hu, X. Liu, Y. Zhang, M. Li, L. Y. Zhang, H. Jin, and L. Wu, “Protecting facial privacy: Generating adversarial identity masks via style-robust makeup transfer,” in *CVPR*, 2022, pp. 15 014–15 023.

[84] S. Hu, J. Zhang, W. Liu, J. Hou, M. Li, L. Y. Zhang, H. Jin, and L. Sun, “Pointca: Evaluating the robustness of 3d point cloud completion models against adversarial examples,” in *Proceedings of the AAAI conference on artificial intelligence*, vol. 37, no. 1, 2023, pp. 872–880.

[85] B. Chen, Y. Feng, T. Dai, J. Bai, Y. Jiang, S.-T. Xia, and X. Wang, “Adversarial examples generation for deep product quantization networks on image retrieval,” *TPAMI*, vol. 45, no. 2, pp. 1388–1404, 2022.

[86] S. Hu, Y. Zhang, X. Liu, L. Y. Zhang, M. Li, and H. Jin, “Advhash: Set-to-set targeted attack on deep hashing with one single adversarial patch,” in *Proceedings of the 29th ACM International Conference on Multimedia*, 2021, pp. 2335–2343.

[87] A. Liu, J. Wang, X. Liu, B. Cao, C. Zhang, and H. Yu, “Bias-based universal adversarial patch attack for automatic check-out,” in *Computer Vision–ECCV 2020: 16th European Conference, Glasgow, UK, August 23–28, 2020, Proceedings, Part XIII 16*. Springer, 2020, pp. 395–410.

[88] X. Yang, F. Wei, H. Zhang, and J. Zhu, “Design and interpretation of universal adversarial patches in face detection,” in *Computer Vision–ECCV 2020: 16th European Conference, Glasgow, UK, August 23–28, 2020, Proceedings, Part XVII 16*. Springer, 2020, pp. 174–191.

[89] Y. Dong, F. Liao, T. Pang, H. Su, J. Zhu, X. Hu, and J. Li, “Boosting adversarial attacks with momentum,” in *CVPR*, 2018, pp. 9185–9193.

[90] N. Papernot, P. McDaniel, S. Jha, M. Fredrikson, Z. B. Celik, and A. Swami, “The limitations of deep learning in adversarial settings,” in *2016 IEEE European symposium on security and privacy (EuroS&P)*. IEEE, 2016, pp. 372–387.

[91] S.-M. Moosavi-Dezfooli, A. Fawzi, and P. Frossard, “Deepfool: a simple and accurate method to fool deep neural networks,” in *CVPR*, 2016, pp. 2574–2582.

[92] A. Madry, A. Makelov, L. Schmidt, D. Tsipras, and A. Vladu, “Towards deep learning models resistant to adversarial attacks,” in *ICLR*, 2018.

[93] S. Fang, J. Li, X. Lin, and R. Ji, “Learning to learn transferable attack,” in *Proceedings of the AAAI Conference on Artificial Intelligence*, vol. 36, no. 1, 2022, pp. 571–579.

[94] Y. Long, Q. Zhang, B. Zeng, L. Gao, X. Liu, J. Zhang, and J. Song, “Frequency domain model augmentation for adversarial attack,” in *ECCV*. Springer, 2022, pp. 549–566.

[95] A. Ilyas, L. Engstrom, A. Athalye, and J. Lin, “Black-box adversarial attacks with limited queries and information,” in *ICML*. PMLR, 2018, pp. 2137–2146.

[96] C. Guo, J. Gardner, Y. You, A. G. Wilson, and K. Weinberger, “Simple black-box adversarial attacks,” in *ICML*. PMLR, 2019, pp. 2484–2493.

[97] L. Li, R. Ma, Q. Guo, X. Xue, and X. Qiu, “Bert-attack: Adversarial attack against bert using bert,” in *Proceedings of the 2020 Conference on Empirical Methods in Natural Language Processing (EMNLP)*, 2020, pp. 6193–6202.

[98] S. Ren, Y. Deng, K. He, and W. Che, “Generating natural language adversarial examples through probability weighted word saliency,” in *Proceedings of the 57th annual meeting of the association for computational linguistics*, 2019, pp. 1085–1097.

[99] J. Gao, J. Lanchantin, M. L. Soffa, and Y. Qi, “Black-box generation of adversarial text sequences to evade deep learning classifiers,” in *2018 IEEE Security and Privacy Workshops (SPW)*. IEEE, 2018, pp. 50–56.

[100] D. Jin, Z. Jin, J. T. Zhou, and P. Szolovits, “Is bert really robust? a strong baseline for natural language attack on text classification and entailment,” in *Proceedings of the AAAI conference on artificial intelligence*, vol. 34, no. 05, 2020, pp. 8018–8025.

[101] A. Kurakin, I. J. Goodfellow, and S. Bengio, “Adversarial machine learning at scale,” in *International Conference on Learning Representations*, 2016.

[102] F. Tramèr, A. Kurakin, N. Papernot, I. Goodfellow, D. Boneh, and P. McDaniel, “Ensemble adversarial training: Attacks and defenses,” *arXiv preprint arXiv:1705.07204*, 2017.

[103] T. Miyato, S.-i. Maeda, M. Koyama, K. Nakae, and S. Ishii, “Distributional smoothing with virtual adversarial training,” *arXiv preprint arXiv:1507.00677*, 2015.

[104] C. Xie, J. Wang, Z. Zhang, Z. Ren, and A. Yuille, “Mitigating adversarial effects through randomization,” in *International Conference on Learning Representations*, 2018.

[105] C. Guo, M. Rana, M. Cisse, and L. van der Maaten, “Countering adversarial images using input transformations,” in *International Conference on Learning Representations*, 2018.

[106] B. Sun, N.-h. Tsai, F. Liu, R. Yu, and H. Su, “Adversarial defense by stratified convolutional sparse coding,” in *CVPR*, 2019, pp. 11 447–11 456.

[107] R. Lu, J. Song, B. Chen, L. Cui, and Z. Wang, “Dagc: Data-aware adaptive gradient compression,” in *INFOCOM*. IEEE, 2023, pp. 1–10.

[108] T. Pang, K. Xu, Y. Dong, C. Du, N. Chen, and J. Zhu, “Rethinking softmax cross-entropy loss for adversarial robustness,” in *International Conference on Learning Representations*, 2019.

[109] A. Mustafa, S. Khan, M. Hayat, R. Goecke, J. Shen, and L. Shao, “Adversarial defense by restricting the hidden space of deep neural networks,” in *ICCV*, 2019, pp. 3385–3394.

[110] M. Mozes, P. Stenetorp, B. Kleinberg, and L. Griffin, “Frequency-guided word substitutions for detecting textual adversarial examples,” in *Proceedings of the 16th Conference of the European Chapter of the Association for Computational Linguistics: Main Volume*, 2021, pp. 171–186.

[111] Y. Zhou, J.-Y. Jiang, K.-W. Chang, and W. Wang, “Learning to discriminate perturbations for blocking adversarial attacks in text classification,” in *Proceedings of the 2019 Conference on Empirical Methods in Natural Language Processing and the 9th International Joint Conference on Natural Language Processing (EMNLP-IJCNLP)*, 2019.

[112] D. Kang, T. Khot, A. Sabharwal, and E. Hovy, “Adventure: Adversarial training for textual entailment with knowledge-guided examples,” in *56th Annual Meeting of the Association for Computational Linguistics, ACL 2018*. Association for Computational Linguistics (ACL), 2018, pp. 2418–2428.

[113] Y. Zhou, X. Zheng, C.-J. Hsieh, K.-w. Chang, and X. Huang, “Defense against adversarial attacks in nlp via dirichlet neighborhood ensemble,” *arXiv preprint arXiv:2006.11627*, 2020.

[114] K. R. Mopuri, A. Ganeshan, and R. V. Babu, “Generalizable data-free objective for crafting universal adversarial perturbations,” *IEEE transactions on pattern analysis and machine intelligence*, vol. 41, no. 10, pp. 2452–2465, 2018.

[115] K. Mopuri, U. Garg, and R. Venkatesh Babu, “Fast feature fool: A data independent approach to universal adversarial perturbations,” in *British Machine Vision Conference 2017, BMVC 2017*. BMVA Press, 2017.

[116] J. Hayes and G. Danezis, “Learning universal adversarial perturbations with generative models,” in *2018 IEEE Security and Privacy Workshops (SPW)*. IEEE, 2018, pp. 43–49.

[117] K. R. Mopuri, U. Ojha, U. Garg, and R. V. Babu, “Nag: Network for adversary generation,” in *CVPR*, 2018, pp. 742–751.

[118] K. R. Mopuri, P. K. Uppala, and R. V. Babu, “Ask, acquire, and attack: Data-free uap generation using class impressions,” in *ECCV*, 2018, pp. 19–34.

[119] Z. Zhou, S. Hu, R. Zhao, Q. Wang, L. Y. Zhang, J. Hou, and H. Jin, “Downstream-agnostic adversarial examples,” in *ICCV*, 2023, pp. 4345–4355.

[120] V. Do, O.-M. Camburu, Z. Akata, and T. Lukasiewicz, “e-snli-ve: Corrected visual-textual entailment with natural language explanations,” *arXiv preprint arXiv:2004.03744*, 2020.

## Appendix A. Pseudocode of the Proposed Algorithm

We present the pseudocode of our proposed attack algorithm for image modality in Alg. 1. Note that the text attacks are completely symmetrical as illustrated in Sec. 4.3.

### Algorithm 1 Pseudocode of universal image attacks

**Require:**  $G_v(\cdot)$ : the perturbation generator;  $D_s$ : the multimodal training set;  $f_I, f_T$ : image encoder and text encoder of the surrogate VLP model;  $N$ : the max iteration;  $\epsilon_v$ : the perturbation budget;  $S$ : the scaling times;  
**Ensure:** Universal image perturbation  $\delta_v$ ;

- 1: **Initialize** the fixed noise  $z_v$  with Gaussian distribution;
- 2: **for**  $i \leftarrow 0$  to  $N$  **do**
- 3:     Randomly sample a image-text data  $(v, t) \sim D_s$ ;
- 4:      $\delta_v = Clip_{\epsilon_v}(G(z_v; t))$ ,  $v_{adv} = v + \delta_v$ ;
- 5:     Augment  $v$  and  $v_{adv}$  into different scales and obtain  $\mathbf{v} = \{v_1 \dots, v_S\}$  and  $\mathbf{v}_{adv} = \{v_1^{adv} \dots, v_S^{adv}\}$ ;
- 6:     Randomly sample a batch of texts from  $D_s$  and obtain  $\mathbf{t}_{pos} = \{t'_1 \dots, t'_K\}$  by selecting the ones with Top-K feature distances from the clean image  $v$ ;
- 7:     Compute  $\mathcal{L}_{CL}$  with  $\mathbf{v}_{adv}$ ,  $\mathbf{t}$  and  $\mathbf{t}_{pos}$  by Eq. (2);
- 8:     Compute  $\mathcal{L}_{dis}$  with  $\mathbf{v}$  and  $\mathbf{v}_{adv}$  by Eq. (3);
- 9:     Compute  $L_{total}$  by Eq. (4);
- 10:    Backward pass and update  $G_v$ ;
- 11: **end for**
- 12: **Return**  $\delta_v$

## Appendix B. Results of the Visual Entailment

Given an image and a textual description, visual entailment involves determining whether the textual description

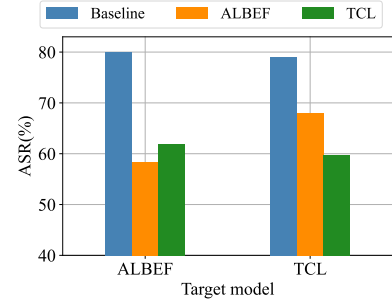


Figure 7. Accuracy of visual entailment under different source models and target models. The Baseline represents the original performance of the target model on the clean data. A higher decrease from the Baseline indicates a better attack performance.

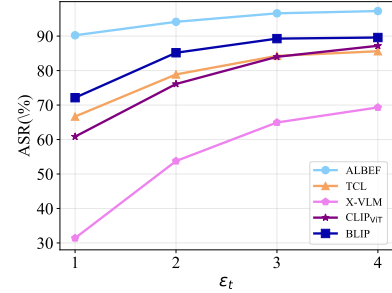


Figure 8. ASR of five target models on the TR task under various values of  $\epsilon_t$ . The surrogate model is ALBEF and the dataset is Flickr30K. As the budget  $\epsilon_t$  increases, the ASR of each target model is also getting higher.

can be inferred from the semantic information of the image. Similar to previous studies [12], [14] on VLP attacks, we conduct experiments on the SNLI-VE [6] dataset using the ALBEF and TCL models. It is notable that [120] has reported a large number of annotation errors in the labels of the SNLI-VE corpus. Therefore, we contend that we do not regard the results of this task as a primary metric for evaluating the efficacy of the attack. Instead, we present the results in Table B for the sake of experimental integrity.

## Appendix C. Textual Perturbation Budget

As expected, the results in Figure 8 show that the perturbation budget  $\epsilon_t$  has an appreciable influence on the attack performance, especially for the black-box adversarial transferability. For instance, when  $\epsilon_t$  increases from 1 to 2, the average black-box attack performance across five models increases significantly by 14.97%. Attackers can adjust the value of  $\epsilon_t$  in accordance with their desires to further enhance the efficacy of the attack while maintaining the perturbation stealthiness.

## Appendix D. More experimental results

We provide the experimental results of cross-domain attacks from Flickr30K to MSCOCO in Table 9. We also present experimental results of the ITR task on R@5 and R@10 in Table 10.

TABLE 9. ASR (%) OF CROSS-DOMAIN ATTACKS FROM FLICKR30 TO MSCOCO.

Source	ALBEF		TCL		X-VLM		CLIP <sub>VIT</sub>		CLIP <sub>CNN</sub>		BLIP	
	TR	IR	TR	IR	TR	IR	TR	IR	TR	IR	TR	IR
ALBEF	<b>97.09</b>	<b>94.87</b>	82.35	77.84	53.02	56.93	77.79	80.15	84.8	86.37	83.43	81.44
TCL	81.84	77.77	<b>97.01</b>	<b>95.61</b>	48.46	53.19	78.33	80.53	84.97	86.29	80.34	78.68
XVLM	60.56	71.58	62.25	71.61	<b>96.48</b>	<b>91.56</b>	78.25	80.75	86.72	88.04	77.43	78.58
CLIP_VIT	67.03	63.66	67.49	63.41	65.75	58.74	<b>95.61</b>	<b>97.03</b>	83.17	85.08	69.94	69.68
CLIP_CNN	52.46	59.52	53.47	60.82	52.5	58.87	63.6	71.37	<b>92.89</b>	<b>93.89</b>	58.7	65.1
BLIP	45.12	54.15	44.87	53.97	36.38	48.04	69.67	74.77	78.67	85.23	<b>93.53</b>	<b>92.58</b>

TABLE 10. ATTACK SUCCESS RATES (%) REGARDING R@5 AND R@10 OF OUR C-PGC AND GAP FOR IMAGE-TEXT RETRIEVAL TASKS.

Dataset	Source	Method	ALBEF		TCL		X-VLM		CLIP <sub>VIT</sub>		CLIP <sub>CNN</sub>		BLIP	
			TR	IR	TR	IR	TR	IR	TR	IR	TR	IR	TR	IR
Flickr30k (R@5)	ALBEF	GAP	59.02	75.47	15.62	17.23	3.4	7.41	18.24	25.34	31.21	38.07	29.88	34.35
		Ours	<b>84.37</b>	<b>80.67</b>	<b>47.05</b>	<b>47.73</b>	<b>10.8</b>	<b>21.89</b>	<b>33.89</b>	<b>50.67</b>	<b>49.26</b>	<b>62.29</b>	<b>54.12</b>	<b>56.59</b>
	TCL	GAP	22.65	23.89	79.39	73.75	3.2	7.25	17.72	26.21	30.57	37.17	25.96	32.62
		Ours	<b>38.58</b>	<b>41.92</b>	<b>91.79</b>	<b>85.12</b>	<b>7</b>	<b>18.25</b>	<b>35.13</b>	<b>51.02</b>	<b>48.3</b>	<b>61.42</b>	<b>42.86</b>	<b>50.03</b>
	XVLM	GAP	13.03	14.72	11.41	14.31	72.3	68.29	20.73	28.88	38.54	43.21	23.44	27.3
		Ours	<b>15.33</b>	<b>32.74</b>	<b>16.42</b>	<b>34.34</b>	<b>90.1</b>	<b>86.31</b>	<b>34.61</b>	<b>49.96</b>	<b>53.29</b>	<b>61.58</b>	<b>38.13</b>	<b>47.24</b>
MSCOCO (R@5)	CLIP_VIT	GAP	11.72	15.37	18.12	20.1	8.2	13.96	71.76	75.2	23.14	37.17	16.5	21.17
		Ours	<b>21.44</b>	<b>27.48</b>	<b>25.43</b>	<b>31.4</b>	<b>15.1</b>	<b>23.69</b>	<b>75.85</b>	<b>85.76</b>	<b>38.11</b>	<b>54.44</b>	<b>26.56</b>	<b>35.85</b>
	CLIP_CNN	GAP	10.03	16.96	15.12	21.63	10.2	16.45	8.7	19.2	60.32	71.91	17.11	23.31
		Ours	<b>11.22</b>	<b>25.65</b>	<b>16.22</b>	<b>32.89</b>	<b>10.8</b>	<b>29.62</b>	<b>16.79</b>	<b>42.13</b>	<b>64.74</b>	<b>74.37</b>	<b>19.32</b>	<b>35.79</b>
	BLIP	GAP	10.32	13.79	11.31	13.55	3.5	7.15	17.1	25.06	28.13	34.92	39.64	68.55
		Ours	<b>24.25</b>	<b>31.34</b>	<b>24.02</b>	<b>31.17</b>	<b>10.3</b>	<b>19.84</b>	<b>32.95</b>	<b>45.41</b>	<b>45.65</b>	<b>57.2</b>	<b>63.48</b>	<b>80.53</b>
MSCOCO (R@5)	ALBEF	GAP	75.51	79.39	39.31	33.28	9.05	10.47	31.87	31.95	41.69	43.44	40.35	39.81
		Ours	<b>93.78</b>	<b>91.98</b>	<b>69.17</b>	<b>63.85</b>	<b>24.98</b>	<b>34.29</b>	<b>57.43</b>	<b>60.91</b>	<b>65.38</b>	<b>69.32</b>	<b>61.29</b>	<b>63.49</b>
	TCL	GAP	44.54	38.39	93.06	88.45	12.02	12.98	33.44	33.58	47.51	47.84	44.38	41.77
		Ours	<b>67.35</b>	<b>63.21</b>	<b>95.24</b>	<b>91.04</b>	<b>31.01</b>	<b>36.68</b>	<b>66.43</b>	<b>72.81</b>	<b>75.09</b>	<b>80</b>	<b>67.63</b>	<b>68.21</b>
	XVLM	GAP	22.94	21.69	23.2	18.9	91.47	83.76	38.49	38.21	58.17	55.32	36.92	34.42
		Ours	<b>40.8</b>	<b>55.13</b>	<b>42.12</b>	<b>53.99</b>	<b>96.95</b>	<b>91.93</b>	<b>63.45</b>	<b>68.48</b>	<b>75.85</b>	<b>78.24</b>	<b>60.78</b>	<b>65.46</b>
Flickr30k (R@10)	CLIP_VIT	GAP	34.27	28.26	37	30.12	32.34	26.51	95.37	93.4	62.99	63.06	35.52	34.64
		Ours	<b>41.59</b>	<b>45.57</b>	<b>42.3</b>	<b>44.05</b>	<b>37.42</b>	<b>40.65</b>	<b>96.76</b>	<b>96.57</b>	<b>71.17</b>	<b>78.14</b>	<b>47.53</b>	<b>53.28</b>
	CLIP_CNN	GAP	27.63	23.83	30.44	25.85	25.67	22.78	24.91	25.34	89.02	<b>90.12</b>	29.46	28.91
		Ours	<b>30.7</b>	<b>38.84</b>	<b>34.22</b>	<b>41.9</b>	<b>30.78</b>	<b>38.67</b>	<b>48.19</b>	<b>56.71</b>	<b>91.95</b>	89.34	<b>37.16</b>	<b>49.6</b>
	BLIP	GAP	19.32	31.08	21.46	26.82	16.58	15.42	37.47	37.28	50.45	50.43	64.68	68.31
		Ours	<b>26.54</b>	<b>34</b>	<b>22.88</b>	<b>32.78</b>	<b>17.21</b>	<b>28.22</b>	<b>52.88</b>	<b>60.74</b>	<b>60.43</b>	<b>68.83</b>	<b>92.46</b>	<b>93.4</b>
MSCOCO (R@10)	ALBEF	GAP	53.9	72.74	11.8	12.13	2	4.63	11.65	17.33	21.78	27.59	23.77	26.52
		Ours	<b>81.5</b>	<b>76</b>	<b>38.3</b>	<b>39.07</b>	<b>7.5</b>	<b>15.38</b>	<b>24.11</b>	<b>40.24</b>	<b>37.83</b>	<b>53.07</b>	<b>46.34</b>	<b>48.02</b>
	TCL	GAP	17.2	17.51	77.1	70.32	2	4.57	12.26	17.84	22.09	28.27	20.16	24.87
		Ours	<b>31.4</b>	<b>33.98</b>	<b>89.6</b>	<b>81.8</b>	<b>5</b>	<b>12.52</b>	<b>24.92</b>	<b>40.94</b>	<b>37.12</b>	<b>52.24</b>	<b>35.81</b>	<b>42.53</b>
	XVLM	GAP	8.4	9.98	8.3	9.34	67.8	63.6	14.39	20.01	30.06	32.83	17.85	20.6
		Ours	<b>11.3</b>	<b>24.61</b>	<b>11.8</b>	<b>26.61</b>	<b>87.3</b>	<b>83.38</b>	<b>25.03</b>	<b>39.61</b>	<b>41.62</b>	<b>51.7</b>	<b>30.99</b>	<b>38.21</b>
MSCOCO (R@10)	CLIP_VIT	GAP	8.4	10.58	12.6	13.73	5.7	9.83	67.3	70.42	17.18	27.86	11.63	15.71
		Ours	<b>15.3</b>	<b>20.28</b>	<b>19.7</b>	<b>23.46</b>	<b>10.8</b>	<b>17.2</b>	<b>67.88</b>	<b>79.55</b>	<b>30.16</b>	<b>45.06</b>	<b>19.86</b>	<b>28.06</b>
	CLIP_CNN	GAP	6.1	11.89	10.1	15.39	7.4	11.22	4.66	12.13	<b>56.56</b>	63.02	11.94	16.64
		Ours	<b>6.8</b>	<b>18.65</b>	<b>10.9</b>	<b>25.22</b>	<b>7.8</b>	<b>23.33</b>	<b>9.83</b>	<b>32.67</b>	54.6	<b>66.58</b>	<b>12.44</b>	<b>27.87</b>
	BLIP	GAP	8.1	9.64	7.3	8.96	2	4.51	10.54	17.09	20.14	25.61	37.61	67.59
		Ours	<b>18.3</b>	<b>24</b>	<b>18.1</b>	<b>23.68</b>	<b>7.6</b>	<b>14.2</b>	<b>22.59</b>	<b>16.13</b>	<b>33.95</b>	<b>47.13</b>	<b>58.88</b>	<b>78.29</b>
MSCOCO (R@10)	ALBEF	GAP	71.1	76.95	32.95	27.27	5.6	7.53	24.82	25.56	34.29	36.41	34.26	35.2
		Ours	<b>91.97</b>	<b>90.21</b>	<b>62.02</b>	<b>56.57</b>	<b>17.46</b>	<b>26.67</b>	<b>48.41</b>	<b>53.65</b>	<b>56.18</b>	<b>62.39</b>	<b>53.51</b>	<b>57.4</b>
	TCL	GAP	37.22	31.34	91.17	85.99	7.64	9.41	26.01	26.83	39.24	40.67	36.86	36.69
		Ours	<b>59.92</b>	<b>56.71</b>	<b>94.31</b>	<b>89.33</b>	<b>23.11</b>	<b>28.9</b>	<b>57.98</b>	<b>66.47</b>	<b>68.09</b>	<b>74.12</b>	<b>59.6</b>	<b>62.68</b>
	XVLM	GAP	17.68	15.88	16.65	13.49	89	80.67	31.31	31.69	50.42	48.25	29.59	28.83
		Ours	<b>31.76</b>	<b>47.04</b>	<b>31.59</b>	<b>45.62</b>	<b>95.23</b>	<b>89.27</b>	<b>55.26</b>	<b>61.65</b>	<b>68.96</b>	<b>72.02</b>	<b>52.73</b>	<b>59.15</b>
MSCOCO (R@10)	CLIP_VIT	GAP	25.96	22.01	28.59	23.65	23.47	20.6	93.91	91.82	57.15	56.49	28.23	28.93
		Ours	<b>32.05</b>	<b>37.64</b>	<b>32.91</b>	<b>36.15</b>	<b>28</b>	<b>33.08</b>	<b>95.81</b>	<b>95.55</b>	<b>64.4</b>	<b>72.94</b>	<b>39.2</b>	<b>46.3</b>
	CLIP_CNN	GAP	20.21	18.05	22.45	20.06	17.75	17.13	18.69	19.87	87.93	<b>86.98</b>	22.7	23.79
		Ours	<b>22.21</b>	<b>31.39</b>	<b>24.89</b>	<b>34.09</b>	<b>21.64</b>	<b>31.59</b>	<b>40.22</b>	<b>49.72</b>	<b>89.42</b>	85.81	<b>30.01</b>	<b>43.09</b>
	BLIP	GAP	12.73	23.96	12.06	20.63	9.63	10.81	30.67	29.89	42.81	42.8	60.09	66.84
		Ours	<b>18.83</b>	<b>26.46</b>	<b>15.49</b>	<b>25.38</b>	<b>10.86</b>	<b>21.92</b>	<b>44.74</b>	<b>53.43</b>	<b>50.42</b>	<b>61.28</b>	<b>90.73</b>	<b>92.46</b>